ISSN 1674-1056
http://cpb.iphy.ac.cn
http://iopscience.iop.org/cpb
中国物理 B
Chinese Physics
中国物理 Chinese Physics B

Nanoscale thermal transport:Theoretical method and application

Yu-Jia Zeng(曾育佳), Yue-Yang Liu(刘岳阳), Wu-Xing Zhou(周五星), Ke-Qiu Chen(陈克求)
Citation: Chin. Phys. B . 2018, 27(3): 036304. **doi:** 10.1088/1674-1056/27/3/036304

Journal homepage: http://cpb.iphy.ac.cn; http://iopscience.iop.org/cpb

What follows is a list of articles you may be interested in

Review of thermal transport and electronic properties of borophene

Dengfeng Li(李登峰), Ying Chen(陈颖), Jia He(何佳), Qiqi Tang(汤琪琪), Chengyong Zhong(钟承勇), Guangqian Ding(丁光前)
Chin. Phys. B . 2018, 27(3): 036303. **doi:** 10.1088/1674-1056/27/3/036303

Improved thermoelectric performance in p-type $Bi_{0.48}Sb_{1.52}Te_3$ bulk material by adding $MnSb_2Se_4$

Binglei Cao(曹丙垒), Jikang Jian(简基康), Binghui Ge(葛炳辉), Shanming Li(李善明), Hao Wang(王浩), Jiao Liu(刘骄), Huaizhou Zhao(赵怀周)
Chin. Phys. B . 2017, 26(1): 017202. **doi:** 10.1088/1674-1056/26/1/017202

Phonon dispersion on Ag (100) surface: A modified analytic embedded atom method study

Xiao-Jun Zhang(张晓军) and Chang-Le Chen(陈长乐)
Chin. Phys. B . 2016, 25(1): 016301. **doi:** 10.1088/1674-1056/25/1/016301

Material properties dependent on the thermal transport in a cylindrical nanowire

Zhang Yong, Xie Zhong-Xiang, Deng Yuan-Xiang, Yu Xia, Li Ke-Min
Chin. Phys. B . 2015, 24(12): 126302. **doi:** 10.1088/1674-1056/24/12/126302

Nature of the band gap of halide perovskites ABX_3 (A= CH_3NH_3, Cs; B= Sn, Pb; X= Cl, Br, I): First-principles calculations

Yuan Ye, Xu Run, Xu Hai-Tao, Hong Feng, Xu Fei, Wang Lin-Jun
Chin. Phys. B . 2015, 24(11): 116302. **doi:** 10.1088/1674-1056/24/11/116302

TOPICAL REVIEW — Thermal and thermoelectric properties of nano materials

Nanoscale thermal transport: Theoretical method and application*

Yu-Jia Zeng(曾育佳), Yue-Yang Liu(刘岳阳), Wu-Xing Zhou(周五星)†, and Ke-Qiu Chen(陈克求)‡

Department of Applied Physics, School of Physics and Electronics, Hunan University, Changsha 410082, *China*

(Received 26 December 2017; revised manuscript received 8 February 2018; published online 13 February 2018)

With the size reduction of nanoscale electronic devices, the heat generated by the unit area in integrated circuits will be increasing exponentially, and consequently the thermal management in these devices is a very important issue. In addition, the heat generated by the electronic devices mostly diffuses to the air in the form of waste heat, which makes the thermoelectric energy conversion also an important issue for nowadays. In recent years, the thermal transport properties in nanoscale systems have attracted increasing attention in both experiments and theoretical calculations. In this review, we will discuss various theoretical simulation methods for investigating thermal transport properties and take a glance at several interesting thermal transport phenomena in nanoscale systems. Our emphasizes will lie on the advantage and limitation of calculational method, and the application of nanoscale thermal transport and thermoelectric property.

Keywords: thermal transport, thermoelectric materials, nanostructure

PACS: 63.22.-m, 72.15.Jf, 61.46.-w **DOI:** 10.1088/1674-1056/27/3/036304

1. Introduction

The size of electronic devices is being reduced to as small as sub-ten nanometer magnitude, and is approaching the feature wavelength of many particle or quasi-particle, such as electron, phonon, and so on. Such small nano-structures exhibit significantly different electronic and thermal properties compared to that of macro ones, and bring us numerous opportunities and challenges. For example, the decreasing device size enables the significant increase of integration degree in integrated circuits, but on the other hand, the enhancement of integration requests better thermal management, including both heat dissipation, heat energy conversion, and so on. These facts make the thermal management an important issue.

Recently, breakthroughs in thermal transport field, such as high-performance thermoelectric materials,[1,2] phonon diode,[3] phonon triode,[4] topological effect of phonon,[5–9] and so on, are emerging endlessly. More excitingly, the rapid development of the synthesis and processing, such as molecular beam epitaxy (MBE)[10] and chemical-vapor deposition (CVD),[11] are enabling the production of devices with well-defined structure and smaller size, and are facilitating the commercial application of these phonon nano-devices.

However, there are still many problems unsolved in this field. For instance, the further application of large-scale power generating by thermoelectric materials is in a dilemma.[12] It is known that most of the energy is dissipated in the form of waste heat. However, the figure of merit (ZT), which describes the thermoelectric energy conversion efficiency, is difficult to improve. Over the past decade, the maximum ZT observed in experiment is still no more than 3,[13] which is far away from mass business application for power generating. On the other hand, the thermal management[14] and near-field heat transport problem[15] have always been plaguing us. The issues of controlling of heat flow, heat dissipation, and heat energy conversion in nanoscale systems have become a specific science field nowadays.[16]

Compared with experiments, the computer simulation has the inherent advantages on researching small size structures. With decreasing further size of devices and emergence of low-dimensional materials, such as graphene,[17] graphene-like structure (MXene,[18] phosphorene,[19] and so on), single molecule junction,[20] and so on, the thermal transport mechanism is different from the macroscopic ones. Fourier's law was proved to be no longer applicable to the anomalous heat transport[21,22] in some nanoscale structures. Fortunately, many new theory models are set up as the powerful tools to study the underlying physics mechanism of nanoscale thermal transport. It is expected to provide a guideline for us to design excellent performance nanoscale devices. The comparison and application range of different theoretical methods is discussed in Section 2. The related thermal transport properties and novel mechanism are presented in Section 3. In Section 4, We focus on the modulation of thermoelectric property and the other mechanism to realize thermoelectric energy conversion.

*Project supported by the Nation Key Research and Development Program of China (Grant No. 2017YFB0701602) and the National Natural Science Foundation of China (Grant No. 11674092).

†Corresponding author. E-mail: wuxingzhou@hnu.edu.cn

‡Corresponding author. E-mail: keqiuchen@hnu.edu.cn

© 2018 Chinese Physical Society and IOP Publishing Ltd

2. Thermal transport theory and calculation method in nanoscale structure

Describing the thermal conductivity accurately is an important issue for the design of nano devices. However, the experiment measurement cannot completely eliminate the impact of the external environment, and the temperature is so difficult to define clearly under the sub-nano size. In recent years, a serial of theoretical methods were proposed, such as the dielectric continuum model,[23] scattering matrix method,[24] molecular dynamics simulation,[25] non-equilibrium Green function method,[26] and Boltzmann transport equation,[27] to predict the thermal conductivity in nanoscale or larger scale. In this section, we mainly introduce different theoretical methods for thermal transport property researches.

2.1. Dielectric continuum model and scattering matrix method

Experimental research has been confirmed that the thermal transport at low temperature and small size is mainly determined by the ballistic process.[28,29] The dielectric continuum model and scattering matrix method were widely used in the study of ballistic thermal transport in low temperature region. Recently, the thermal conductivity of various low-dimensional systems, such as abrupt structures,[30,31] rough surfaces,[32] defects,[33] and stub structure,[34,35] have been widely studied by these methods.

In long wavelength limit, the dielectric continuum model is a reasonable approximation to study the thermal transport property on the condition that the structure is continuous and compact, and if the wavelength is larger than the size of materials, the structure of inner system can be ignored. In this model, the stress, strain, and displacement are functions of continuous coordinate so that the conception of continuous and limitation applied in mathematic deduction is so convenient. In past few years, the dielectric continuum model was widely used to study the thermal transport property in nanostructure at low temperature, such as supperlattice[36,37] and wave-guide structure.[38] At low temperature, only several acoustic phonons were excited in system so that the dielectric continuum model provides sufficient accuracy for the research of thermal transport. In this model, the wave equation of the entire system can be defined as

$$\rho \frac{\partial^2 \psi}{\partial t^2} = C\nabla^2 \psi, \tag{1}$$

where ψ is the wave function of phonon, ρ is the density of materials, and C is the elastic constant of the materials. We assume that the cross-section of materials is rectangle and the transport direction is x. The width of y and z is denoted as W_1 and W_2, respectively. The wave equation can be solved by variables separation and further expressed as

$$\psi(x,y,z) = \sum_{m=0}\sum_{n=0}[A_{nm}\mathrm{e}^{\mathrm{i}k_{nm}x} + B_{nm}\mathrm{e}^{-\mathrm{i}k_{nm}x}]\phi_{mn}(y,z), \tag{2}$$

where A_{nm} and B_{nm} are undetermined coefficients, and $\phi_{mn}(y,z) = \phi_m(x)\phi_n(z)$. The relation between them will be consistent with the dispersion relations

$$k_{nm} = \sqrt{\frac{\omega^2}{v^2} - \frac{m^2\pi^2}{W_1^2} - \frac{n^2\pi^2}{W_2^2}}, \tag{3}$$

where k_{nm} is the wave vector, v is the longitudinal velocity of phonon, m and n are phonon index, which denote the propagation mode and decay mode when k_{nm} is a real number and imaginary number respectively. If the stress free boundary $(\hat{n}\cdot\nabla\psi)|_{y=W_1,z=W_2} = 0$ is used in the interface of materials, the lateral wave function can be expressed as

$$\phi_m = \begin{cases} \sqrt{\dfrac{2}{W_1}}\sin\left(\dfrac{m\pi y}{W_1}\right), & m = 1,3,5,\ldots \\ \sqrt{\dfrac{2}{W_1}}\cos\left(\dfrac{m\pi y}{W_1}\right), & m = 2,4,6,\ldots \\ \sqrt{\dfrac{1}{W_1}}, & m = 0, \end{cases} \tag{4}$$

$$\phi_n = \begin{cases} \sqrt{\dfrac{2}{W_2}}\sin\left(\dfrac{n\pi y}{W_2}\right), & n = 1,3,5,\ldots \\ \sqrt{\dfrac{2}{W_2}}\cos\left(\dfrac{n\pi y}{W_2}\right), & n = 2,4,6,\ldots \\ \sqrt{\dfrac{1}{W_2}}, & n = 0. \end{cases} \tag{5}$$

On the contrary, if we adopt hard-wall boundary $\psi|_{y=W_1,z=W_2} = 0$ in the interface of materials, the wave function will be expressed as

$$\phi_m = \begin{cases} \sqrt{\dfrac{2}{W_1}}\sin\left(\dfrac{m\pi y}{W_1}\right), & m = 1,3,5,\ldots \\ \sqrt{\dfrac{2}{W_1}}\cos\left(\dfrac{m\pi y}{W_1}\right), & m = 2,4,6,\ldots \end{cases} \tag{6}$$

$$\phi_n = \begin{cases} \sqrt{\dfrac{2}{W_2}}\sin\left(\dfrac{n\pi y}{W_2}\right), & n = 1,3,5,\ldots \\ \sqrt{\dfrac{2}{W_2}}\cos\left(\dfrac{n\pi y}{W_2}\right), & n = 2,4,6,\ldots \end{cases} \tag{7}$$

From the above results, we can obtain the dispersion relations

$$\omega^2 = \omega_{mn}^2 + k_{mn}^2 v^2. \tag{8}$$

When a suitable boundary condition and interface roughness were given, the transmission coefficient of corresponding regions can be obtained by transfer matrix or scattering matrix method so as to get the thermal conductance of the materials.

The scattering matrix is a processing method on the basis of the dielectric continuum model. In general, the transfer matrix and scattering matrix method are both in common use to solve the transport problem of periodic or quasi-periodic quantum structures. The probability distribution of particle in any position can be easily obtained by transfer matrix. However,

because the retard mode inevitably increases with the exponent, and result in singularity of transfer matrix, so that the transfer matrix method cannot describe the complex shaped and larger size difference structure. Compared with the transfer matrix method, the scattering matrix method not only have the benefit of the transfer matrix method, but also overcome the disadvantage of transfer matrix method. Therefore, it is more suitable to deal with the particle transport problem in complex structure.

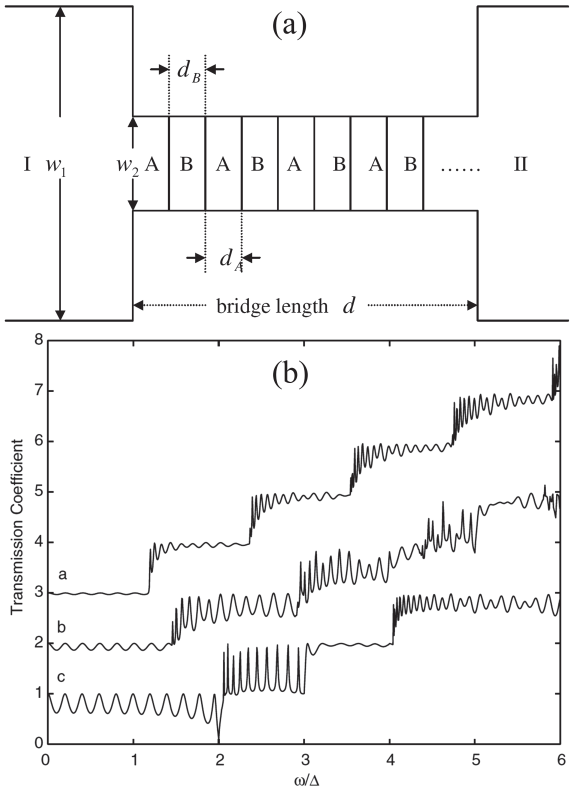


Fig. 1. (a) Regions I and II, with width ω_1 and ω_2 respectively, which are connected by the bridge with length d. The bridge consists of a finite repetition of alternating layers of material A with thickness $d_{\rm A}$ and materials B with thickness $d_{\rm B}$. (b) A typical transmission coefficient as a function of ω/Δ calculate by scattering matrix method. Reprinted with permission from Ref. [24]. Copyright (2003) by IOP Publishing.

An example was given here, the structure scheme is show in Fig. 1(a), based on dielectric continuum model, in stress-free boundary, the wave function in different area, lateral wave function, and dispersion relations are given by

$$\psi^{\gamma}(x,y) = \sum_{m=0}^{M^{\gamma}} [A_{\gamma}^{m} \mathrm{e}^{\mathrm{i}k_m^{\gamma}(x-x_{\gamma})} + B_m^{\gamma} \mathrm{e}^{-\mathrm{i}k_m^{\gamma}(x-x_{\gamma})}]\phi_m^{\gamma}(y), \quad (9)$$

$$\phi_n^{\gamma}(y) = \begin{cases} \sqrt{\dfrac{2}{\omega}} \cos\left(\dfrac{n\pi y}{\omega}\right), & n = 1,3,5,\ldots \\ \sqrt{\dfrac{2}{\omega}} \sin\left(\dfrac{n\pi y}{\omega}\right), & n = 2,4,6,\ldots \end{cases} \quad (10)$$

$$k_m^{\gamma} = \sqrt{\frac{\omega^2}{v_{\gamma}^2} - \frac{m^2\pi^2}{W_{\gamma}^2}}. \quad (11)$$

Here, we simply set $\gamma = \mathrm{I},\mathrm{II}$ in Eq. (9) to label different regions of this structure, and different regions can be connected by the following equations:

$$\begin{pmatrix} \boldsymbol{B}^{\mathrm{I}} \\ \boldsymbol{A}^{\mathrm{II}} \end{pmatrix} = \boldsymbol{S}(\mathrm{I},\mathrm{II}) \begin{pmatrix} \boldsymbol{A}^{\mathrm{I}} \\ \boldsymbol{B}^{\mathrm{II}} \end{pmatrix}. \quad (12)$$

We can simplify the form of $\boldsymbol{S}$ matrix by the condition that ψ and ψ' will be continuous on the boundary so that the corresponding scattering matrix of different region can obtained. However, the derivation process is complicated and we skip this step in this paper, the expression of $\boldsymbol{S}$ matrix can written as

$$\boldsymbol{S}(I,I) = \begin{pmatrix} 0 & \boldsymbol{P} \\ \boldsymbol{P} & 0 \end{pmatrix}, \quad (13)$$

where $\boldsymbol{P}$ is a N-dimensional diagonal matrix with diagonal elements $P_{nn} = \mathrm{e}^{\mathrm{i}k_n^j d_j}$, d is the longitudinal dimension. The expansion coefficients of the phonon wave function in regions I and II are correlated through the total scattering matrix

$$\begin{aligned} \begin{pmatrix} \boldsymbol{B}^{\mathrm{I}} \\ \boldsymbol{A}^{\mathrm{II}} \end{pmatrix} &= \boldsymbol{S}(\mathrm{I},\mathrm{II}) \begin{pmatrix} \boldsymbol{A}^{\mathrm{I}} \\ \boldsymbol{B}^{\mathrm{II}} \end{pmatrix} \\ &= \begin{pmatrix} \boldsymbol{S}_{11}(\mathrm{I},\mathrm{II}) & \boldsymbol{S}_{12}(\mathrm{I},\mathrm{II}) \\ \boldsymbol{S}_{21}(\mathrm{I},\mathrm{II}) & \boldsymbol{S}_{22}(\mathrm{I},\mathrm{II}) \end{pmatrix} \begin{pmatrix} \boldsymbol{A}_{\mathrm{I}} \\ \boldsymbol{B}_{\mathrm{II}} \end{pmatrix}. \end{aligned} \quad (14)$$

The total scattering matrix of the quantum structure can be constructed by the composition of the individual scattering matrices associated with each sub region

$$\begin{aligned} \boldsymbol{S}(\mathrm{I},\mathrm{II}) \;=\; & \boldsymbol{S}(\mathrm{I}, j=1) \otimes \left[\prod_{j}^{M-1} S(j,j) \otimes S(j,j+1) \right] \\ & \otimes \boldsymbol{S}(j=M,\mathrm{II}). \end{aligned}$$

In the appropriate boundary condition, we can obtain

$$\begin{pmatrix} \boldsymbol{A}_{\mathrm{I}} \\ \boldsymbol{B}_{\mathrm{II}} \end{pmatrix} = \begin{pmatrix} I_l \\ 0 \end{pmatrix}. \quad (15)$$

Inserting this boundary condition into Eq. (14), we obtain

$$\begin{pmatrix} \boldsymbol{B}^{\mathrm{I}} \\ \boldsymbol{A}^{\mathrm{II}} \end{pmatrix} = \begin{pmatrix} \boldsymbol{S}_{11}(\mathrm{I},\mathrm{II}) & \boldsymbol{S}_{12}(\mathrm{I},\mathrm{II}) \\ \boldsymbol{S}_{21}(\mathrm{I},\mathrm{II}) & \boldsymbol{S}_{22}(\mathrm{I},\mathrm{II}) \end{pmatrix} \begin{pmatrix} I_l \\ 0 \end{pmatrix}. \quad (16)$$

The coefficient vectors $\boldsymbol{A}^{\mathrm{II}}$ and $\boldsymbol{B}^{\mathrm{I}}$ can be obtained from the following equations:

$$\boldsymbol{A}^{\mathrm{II}} = \boldsymbol{S}_{21}(\mathrm{I},\mathrm{II}) I_l, \quad (17)$$

$$\boldsymbol{B}^{\mathrm{I}} = \boldsymbol{S}_{11}(\mathrm{I},\mathrm{II}) I_l. \quad (18)$$

The flux transmission and reflection probability from incident mode m in region I to final mode n in region II are give by

$$\widetilde{t}_{mn} = |t_{mn}^2| \frac{k_n^{\mathrm{II}}}{k_m^{\mathrm{I}}}, \quad (19)$$

$$\widetilde{r}_{mn} = |r_{mn}^2| \frac{k_n^{\mathrm{II}}}{k_m^{\mathrm{I}}}. \quad (20)$$

We can easily get the transmission coefficient of individual incident mode m in region I by sum the propagation modes in region II

$$\tau_m(\omega) = \sum_{n,\omega_m<\omega} \widetilde{t}_{mn}. \quad (21)$$

As shown in Fig. 1(b), the total transmission probability is calculated by

$$\tau = \sum_{n,\omega_n<\omega} \tau_m(\omega). \tag{22}$$

Once obtained the transmission coefficient, we can get the thermal conductance by following equation:

$$\sigma = \frac{\hbar^2}{k_B T^2} \sum_m \frac{1}{2\pi} \int_{\omega_m}^{\infty} \tau_m(\omega) \frac{\omega^2 \exp\left(\frac{\hbar\omega}{k_B T}\right)}{\left[\exp\left(\frac{\hbar\omega}{k_B T}\right) - 1\right]^2} \mathrm{d}\omega. \tag{23}$$

Consider the limit of the paper, we only give the main ideal of dielectric continuum model and scattering method, and the detail discussion of scattering matrix method can refer to Refs. [24], [33], and [36]. It is worth noting that the elastic continuum model is just applicable to the long wavelength limit, in which the phonon wavelength was much larger than the lattice constant of materials, so that only the low temperature can be considered in this method. At higher temperature, the phonon wavelength will be more shorter, so that we could no longer afford to ignore the diffuse thermal transport process. At this time, the elastic continuum model needs to be reassess.

2.2. Non-equilibrium Green function method

The non-equilibrium Green function (NEGF) method originates mainly from the quantum field theory. In general, this method were used to study the ballistic transport of electron and phonon in nanoscale, also the phonon–phonon interaction[39,40] and electron–phonon coupling[41] can be considered. However, the amount of computing is so huge that it cannot be done well with the current computing power. Therefore, we only discuss the linear part of Green's function method in this review. Considering a two-probe model that is compose by three parts, i.e., the left semi-infinite region (L), the central scattering region (C), and the right semi-infinite region (R), the Hamiltonians of entire system can be written as

$$H_{\mathrm{sys}} = \sum_{\alpha=\mathrm{L.C.R}} H_\alpha + (u^{\mathrm{L}})^{\mathrm{T}} V^{\mathrm{LC}} u^{\mathrm{C}} + (u^{\mathrm{C}})^{\mathrm{T}} V^{\mathrm{CR}} u^{\mathrm{R}} + H_n, \tag{24}$$

where the H_α is the total energy, u^α is the lattice displacement vector of region α, the V^{LC} and V^{CR}, is coupling matrix of left and right leads to the central region. The H_α is given by the following equation:

$$H_\alpha = \frac{1}{2}(\dot{u}^\alpha)^{\mathrm{T}} \dot{u}^\alpha + \frac{1}{2}(u^\alpha)^{\mathrm{T}} \boldsymbol{K}^\alpha u^\alpha, \quad (\alpha = \mathrm{L,C,R}). \tag{25}$$

$\boldsymbol{K}^\alpha$ is the force constant matrix, which is derived by empirical force field (EFF) or density functional theory (DFT), and the former will be more faster than later in calculation. For a linear system $\boldsymbol{K}^\alpha$ can be written as

$$\boldsymbol{K} = \begin{pmatrix} K^{\mathrm{L}} & V^{\mathrm{LC}} & 0 \\ V^{\mathrm{CL}} & K^{\mathrm{C}} & V^{\mathrm{CR}} \\ 0 & V^{\mathrm{RC}} & K^{\mathrm{R}} \end{pmatrix}. \tag{26}$$

At low temperature, the lattice vibration is a slight vibration problem, the transport process can be approximated to harmonic ($H_n = 0$) so that the nonlinear interaction in the central region is ignored generally in many studies.[42–46] Utilizing this hamiltonian system, the retarded surface Green's function for the center region and left/right region can be calculated by

$$g_\alpha^{\mathrm{r}} = [(\omega + \mathrm{i}\eta)^2 I - K^\alpha]^{-1}, \quad (\alpha = \mathrm{L,R}). \tag{27}$$

After obtaining the surface Green's function of the leads, the retarded self-energy of the leads can be given by

$$\Sigma_\alpha^{\mathrm{r}} = V^{\mathrm{C}\alpha} g_\alpha^{\mathrm{r}} V^{\alpha\mathrm{C}}, \tag{28}$$

where $\Sigma_\alpha^{\mathrm{r}}$ and g_α^{r} are the self-energy and surface green function in region α, respectively. It contains the coupling information between the left/right region and the center region. The spread function of central scattering region and heat source can be defined by the following equation:

$$\Gamma_\alpha = \mathrm{i}(\Sigma_\alpha^{\mathrm{r}} - \Sigma_\alpha^{\mathrm{a}}) = -2\,\mathrm{Im} V^{\mathrm{C}\alpha} g_\alpha^{\mathrm{r}} V^{\alpha\mathrm{C}}. \tag{29}$$

Then, the retarded Green's function of central scattering region can be expressed as

$$G^{\mathrm{r}} = G_{\mathrm{CC}} = [(\omega + \mathrm{i}\eta)^2 I - K^{\mathrm{C}} - \Sigma_{\mathrm{L}}^{\mathrm{r}} - \Sigma_{\mathrm{r}}^{\mathrm{R}}]^{-1}. \tag{30}$$

From above, the phonon transmission coefficient $T(\omega)$ and phonon density of state $\rho(\omega)$ are given by

$$T(\omega) = \mathrm{Trace}(G^{\mathrm{r}} \Gamma_{\mathrm{L}} G^{\mathrm{a}} \Gamma_{\mathrm{R}}), \tag{31}$$

$$\rho(\omega) = \frac{\mathrm{i}\omega}{\pi} \mathrm{Trace}(G^{\mathrm{r}} - G^{\mathrm{a}}). \tag{32}$$

Accordingly, we can simply express the phonon thermal conductance in a form similar to the Landauer formula for the ballistic transport as follows:

$$\kappa_{\mathrm{ph}} = \frac{1}{2\pi} \int \hbar\omega T(\omega) \frac{\partial f(\omega, T)}{\partial T} \mathrm{d}\omega, \tag{33}$$

where $f(\omega, T)$ is the Bose–Einstein distribution for phonon at the frequency ω and absolute temperature T. As a comparison, Peng *et al.*[47] compared the difference of force constant model and dielectric continuum model. In conclusion, as shown in Fig. 2, the result shows that the phonon transmission spectra display different characters in higher frequency region in the two models and similar stepwise in low-frequency region so as to result in a bigger thermal conductance in higher temperature region, but present a similar behavior in quantum structure at low temperature.

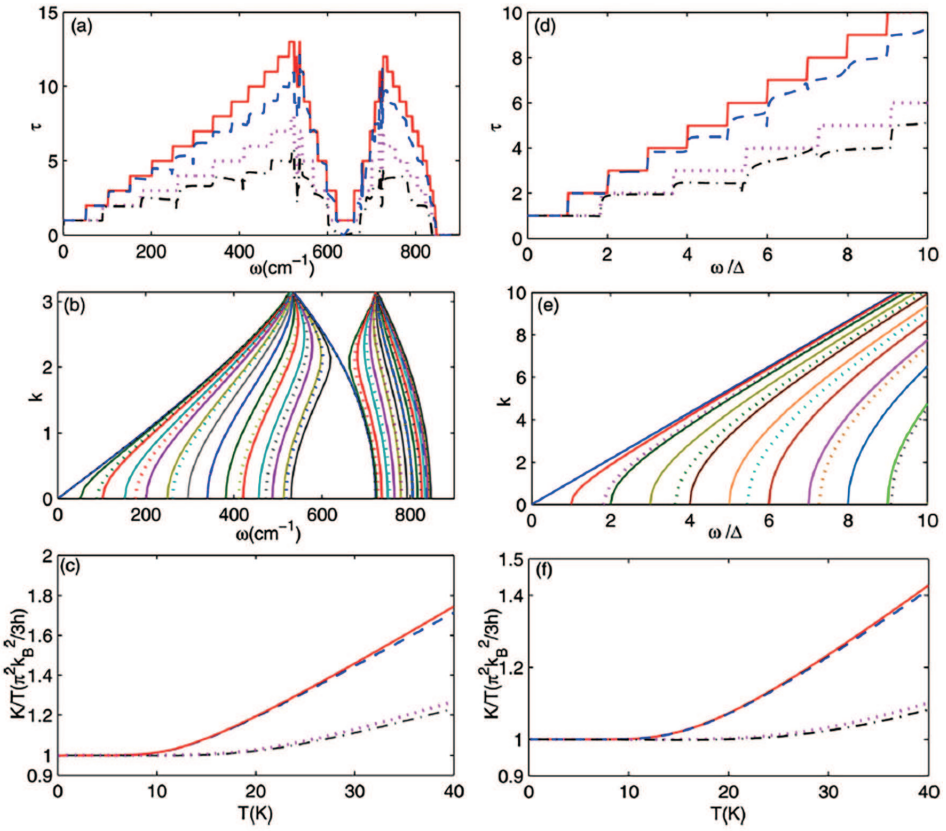


Fig. 2. (color online) (a), (d) Phonon transmission function of out-of-plane modes and horizontally polarized SH mode calculate by force-constant model and dielectric continuum model, respectively. The different curve represent the 14-ZGNR without defect (solid line), with double-cavity defect (dashed line), and the 8-ZGNR without defect (dotted line), with double-cavity defect (dash-dotted line), respectively. (b), (e) The phonon dispersion relation of 14-ZGNR (solid curve) and 8-ZGNR (dotted curve) without double cavity. (c), (f) The corresponding total thermal conductance divided by temperature K/T. Reprinted with permission from Ref. [47]. Copyright (2011) by AIP Publishing LLC.

2.3. Molecular dynamics

In small size and low temperature limitation, only the acoustic modes are excited in system so that the dielectric continuum model is an efficient method to calculate thermal conductance. However, there are some non-physics caused by dielectric continuum approximation, such as infinite mean-free-path of phonon, different phonon thermal conductivity, zero temperature gradient, etc. In fact, if the size of materials close to the mean free path of phonon, the heat transport process is not only ballistic but also diffuse, it is the combination of both ballistic and diffuse,[48] and the phonon–phonon interaction is objective existed in a real system so that the expansion of potential energy must be considered to higher order terms in thermal transport research.

The molecular dynamics simulation, which can take the anharmonic effect into account, has been risen up as a powerful tool in recent years for the researching of thermal conductivity and frequency dependent thermal property. Compared with the previous method as is discussed in above, MD method based on force field (FF) which can get more information without any initial physical environment settings. Because of that, the molecular dynamics simulation is an ideal method for investigating the fundamental thermal property for complex structure[49–53] and various structure dependent property.[54–59] In addition, the MD simulation can also be used in liquids,[60] surfaces,[61,62] clusters,[63–65] topological insulators,[66] and so on.

There are two different methods to research the heat transport properties in molecular dynamics simulation, i.e., the non-equilibrium (NEMD) and the equilibrium molecular dynamics (EMD), respectively. The NEMD method is also known as the direct method, which is based on the Fourier's law to calculate thermal conductivity. For the non-equilibrium method, by introduced a temperature gradient into the both ends of the entire system artificially, the heat flux will be constructed when the entire system tends to the statistic non-equilibrium steady state. The temperature of relative columns atom along the longitudinal of materials is defined by energy equipartition theorem, and the thermal conductivity can be simply obtained by Fourier's laws

$$J = -\kappa \nabla T. \tag{34}$$

This method is more similar to real experiment measurement; it is consistent with the actual physics process of heat conduction. More importantly, the way to control temperature such as the Langevin thermostat, which is based on Brownian dynamics, is a well-known motion laws of microscopic particle, and is consistent with the fluctuation-dissipation theory. However,

the shortcoming of NEMD method is the artificial heat bath. For the Nose–Hoover thermostat,[67,68] the nonlinear response of heat source and heat sink will result in fluctuation of heat flux so that the nonequilibrium steady state is difficult to obtain. For the Langevin thermostat,[69] the damping parameter λ will be hugely influence temperature distribution. A smaller λ results in the temperature being so difficult to reaching expect value, and a stronger λ will give rise to a large temperature jumping at the boundary of thermostate.

To calculate intrinsic thermal conductivity of materials, the EMD method will be more suitable. Because there is not any artificial heat bath introduced into the entire simulation system. In short, the EMD method is based on Green–Kubo formula[70,71] originating from fluctuation-dissipation theory. It can be defined as follows:

$$K = \frac{1}{3Vk_{\mathrm{B}}T^2}\int_0^{\tau_{\mathrm{m}}} \langle J(t)J(0)\rangle \,\mathrm{d}t, \tag{35}$$

where V is volume, k_{B} is Boltzmann constant, T is average temperature, τ_{m} is correlation time, and $J(t)J(0)$ is heat flux auto-correlation function. It is worth noting that both the NEMD and EMD methods, which are based on the classic Newton's law, can not take quantum effect into consideration. Therefore, the MD method cannot reproduce the well-known quantization thermal conductance at low temperatures and quantum structure. To remedy the shortcoming of MD method, as a post-processing step after MD simulation, the quantum correction technique can be appropriately expressing temperature effect in MD simulation,[72] which assumes that the heat flux is equal in the classical and quantum system. The thermal conductivity can be redefined by quantum correction as follows:

$$\kappa_{\mathrm{real}} = \kappa_{\mathrm{MD}}\frac{\partial T_{\mathrm{MD}}}{\partial T_{\mathrm{real}}}. \tag{36}$$

Although the discrepancy of classical temperature and quantum temperature can be corrected by equating the total energy in classical and quantum descriptions. However, the actual microscopic dynamics and mechanical property at low temperatures is still unable to reproduce by this method so that there is a huge discrepancy between MD simulation and fully quantum approach in the calculation of thermal conductivity below Debye temperature. Another quantum approximation has been proposed to mitigate this limitation in classical molecular dynamics system, such as the quantum Langevin heat bath technology, and the detail can be seen in Refs. [73] and [74].

2.4. Boltzmann transport theory

For the larger size materials, according to dynamics theory, the lattice vibration can be approximate to phonon gas, which satisfies with the Bose–Einstein distribution. The advantage of this method is the various nonlinear transport processes, such as the Umklapp process, electron–phonon coupling, can be considered in calculation. If the phonon distribution function in non-equilibrium state is little difference with the the equilibrium state so that we can simply regard the phonon scattering process as the phonon relaxation time. In general, we can use Fermi's golden rule to obtain all phonon scattering rate.[75,76] However, the ultra-high computing cost makes the scattering rate of different phonon modes so difficult to obtain. Hence, we can simplify the solution by relaxation time approximation. Usually, there are four different kinds of phonon scattering processes:[77–80] three-phonon scattering, impurity scattering, boundary scattering, and the electron–phonon scattering. Based on Matthiessen's rule and without considering the coupling relations between them, the total relaxation time can be written as

$$\tau^{-1} = \tau_{\mathrm{U}}^{-1} + \tau_{\mathrm{i}}^{-1} + \tau_{\mathrm{B}}^{-1} + \tau_{\mathrm{ep}}^{-1}. \tag{37}$$

If the temperature gradient is along the α direction, in specify boundary, the heat flux density is given by

$$J_\alpha = \sum_k N_\lambda \hbar\omega_\lambda v_\lambda^\alpha = \int N_\lambda \hbar\omega_\lambda v_\lambda^\alpha \rho(\omega)\,\mathrm{d}\omega, \tag{38}$$

where v_λ^α is the group velocity of α component, $\rho(\omega)$ is the phonon density of state. Then, combining Eq. (38) and Fourier's law, we can obtain the phonon thermal conductivity

$$\kappa = \frac{1}{3}C_v v^2 \tau, \tag{39}$$

where C_v is the specific heat capacity, for a linear dispersion relations $\omega_\lambda = v\lambda$, according to Deybe model, the distribution of different phonon to thermal conductivity can be expressed as

$$\kappa = \frac{k_{\mathrm{B}}}{2\pi^2 v}\left(\frac{k_{\mathrm{B}}}{\hbar}\right)^3 T^3 \int_0^{\theta_{\mathrm{D}}/T} \tau(\beta)\frac{\beta^4}{(\mathrm{e}^\beta - 1)^2}\,\mathrm{d}\beta, \tag{40}$$

$$\beta = \frac{\hbar\omega}{k_{\mathrm{B}}T}, \tag{41}$$

where θ_{D} is Deybe temperature. However, to accurately solve the Boltzmann transport equation requires that the researcher have pre-knowledge for physical process of phonon scattering. Moreover, the fluctuation of phonon was ignored in this method, there are many researches demonstrated that when the size of material is comparable with the phonon wavelength, the standing wave and phonon coherent phenomenon will be observed. For a brief conclusion, the application range of different methods have limitation at present. It is very important to choose appropriate method to study different problems in nanoscale. We simply summarized the advantages and disadvantages of different method in Table 1.

Table 1. Comparison of different calculation method for thermal transport.

Method	Theoretical basis	Advantage	Disadvantage	Application range
Nonequilibrium Green's function	Quantum theory	Quantum effect	Anharmonic effect	10–10^3 atoms
Scattering Matrix	Dielectric continuum model	Quantum effect	Atomic interaction	Mesoscopic
Molecular Dynamics	Newton's equation	Anharmonic effect	Quantum effect	10^3–10^8 atoms
Boltzmann Transport Equation	Semi-classical Quantum theory	Anharmonic effect	Wave behavior of phonon	Periodic structure

3. Thermal transport property in nanoscale structures

With the increasing ICs chips integration level and the device size shrinks, the thermal management has become an extremely urgent issue. It is important to find the ultra-high thermal conductivity materials to serve as the heat dissipation or conduct device. But on the other hand, the ultra-low thermal conductivity materials, which can be used in thermoelectric cooling or energy conversion, are also a ways to solve these problems. All these problem requires an efficient way to control heat flow in nanoscale. Because of that, the in-depth understanding of thermal property of various materials is directly relates to the lifetime of electronic device and energy conversion efficiency. In this section, we would like to give a brief review on the thermal property of various nanostructure and novel physical mechanisms from the theoretical simulation standpoint.

Unlike the bulk materials, the low dimensional structure, such as graphene, will be hugely influenced by quantum confinement effect. It has drawn great attention in recent years due to the unique physical properties, such as the robust negative differential resistance phenomena,[81] excellent mechanical property,[82] ultra-high thermal conductivity,[83–85] and quantum anomalous Hall effect,[86] and so on. Moreover, other graphene-like materials, such as MoS_2,[87] graphyne,[88] borophene,[89] silicene,[90] etc., were emerging endlessly. These discoveries make possible to understand the thermal transport mechanism in nanoscale.

For 2D materials, there are various factors can influencing the thermal conductivity significantly,[91] such as size,[92] defect and doping,[93,94] edge,[95] substrate,[96] and so on. In general, the high-frequency phonon will be greatly influenced by defects and impurities,[97,98] while the low-frequency phonons are insensitive to these kinds of effect.[99] However, the previous works does not take the different phonon modes into account. Utilizing the NEGF method, Peng *et al.*[100] described the influence of different types defect for thermal conductivity of graphene nanoribbon. It is found that different vibration modes will show different behaviors on different defect sizes and types, as shown in Fig. 3.

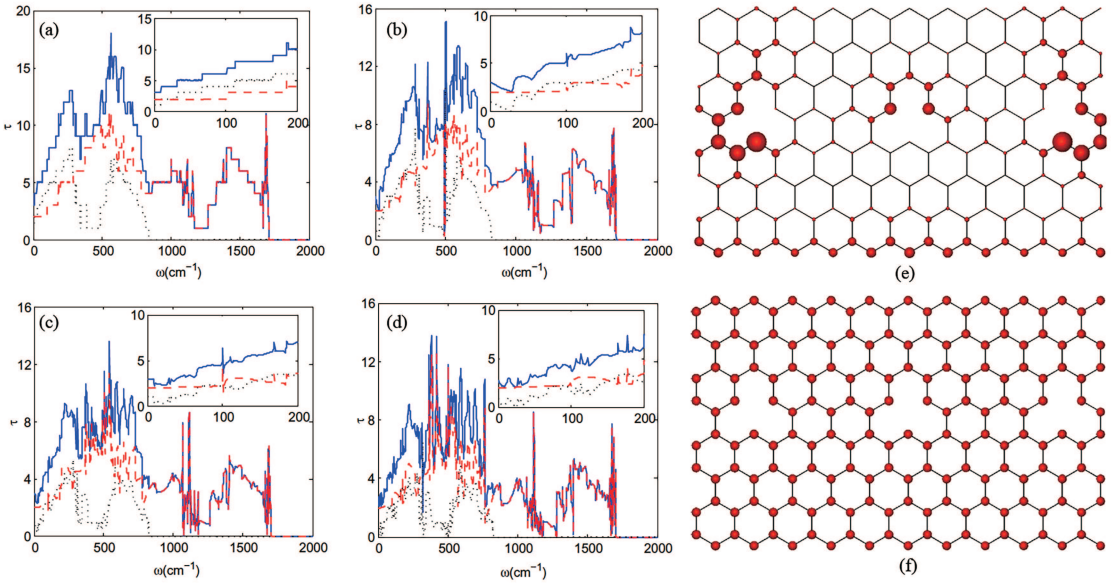


Fig. 3. (color online) Phonon transmission function of 8-ZGNR: (a) without cavity; (b) with a cavity; (c) with two cavities; (d) with three cavities, respectively. Different curves corresponding to the total transmission rate (blue solid line), transmission rate of IPMs (red dashed line), and transmission rate of FPMs (black dotted line), respectively. (e), (f) Phonon local density of state of the (e) FPMs and the (f) IPMs at $\omega = 25$ cm^{-1}. Reprinted with permission from Ref. [100]. Copyright (2014) by Elsevier Publishing.

Interestingly, the two kinds of phonon modes show different characteristics in cut-off frequency after we separate the phonon transmission spectrum into out-of-plane and in-plane vibration. The further result shows that the flexural phonon modes (FPMs), especially the high-frequency region, is more influenced by cavity defect, which agrees well with previous works. More interestingly, for the IPMs (in-plane phonon modes) the low-frequency phonon is no longer sensitive to the cavity defect, and even the high-frequency phonon has also almost not affected by this defect type. From the perspective of the phonon density of state, the difference of FPMs and IPMs will be more obvious. The FPMs is totally localized at the frequency 25 cm^{-1}. This indicates that the low-frequency phonon influenced by vacancy defect on graphene and other 2D materials may be also strongly associated with the shape of the defect rather than only the high frequency phonon will be influenced by vacancy defect.

With the dimension further decreasing, the quantum effect will affect the physical property of materials more strongly. Before the discovering of graphene, the one/zero dimensional nano structure have been observed by many experimental researches. The thermal property of nanowire,[101,102] nanotube,[103–106] quantum dot[107] and another shaped quantum structure[108] has been attracted increasing attention in recent years. Many interesting physical phenomena associate with these structures were observed by theoretical simulation and experiment, such as the anomalous heat conduction,[109] phonon-assisted heat generation,[110] splitting behavior of acoustic phonon,[111] reversal of thermal rectification,[112] and so on. For these structures, due to the size of device is much smaller than mean free path of phonon so that the scattering matrix method and nonequilibrium Green's function method can be more convenient to describe the transmission coefficient of different phonon modes, which consist well with the experimental result in low temperature. Like the spectroscope, the theoretical simulation can easily separate the different phonon modes contribution of thermal conductance so that to study the underlying physical mechanism of thermal transport, and this is usually unattainable in experiment measurements.

Figure 4(a) shows a GaAs catenoidal structure quantum wire,[113] and the thermal conductance of different types of vibrational modes was little attention in this structure. As shown in Figs. 4(b)–4(d), the thermal transport behavior shows different behavior with different structure. An obvious quantized thermal conductance plateau can be observed in the perfect quantum wire, and the two optical modes are coupling with each other in perfect quantum wire so that to be distinguishing them is so difficult. For catenoidal structure quantum wire, the different transport behavior of different vibrational modes can be found between optical mode and acoustic mode, and the result shows that the universal quantized thermal conductance value $\pi^2 k_B^2 T/3h$ at low temperature originates from the lowest four acoustic modes so that we can only observe four units of the value $\pi^2 k_B^2/3h$, and a previous theoretical research also confirmed this result.[114] Moreover, it can be simply seen that the single acoustic mode is more sensitive to the variation in the structure parameters.

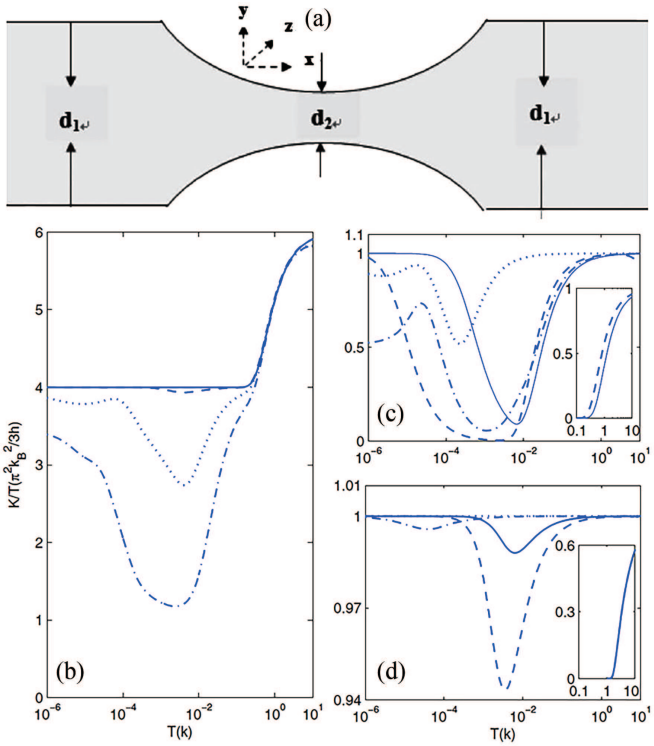


Fig. 4. (color online) (a) Heat source and heat sink with the temperature T_1 and T_2 are connected by a catenoidal wire with a rectangular cross-sectional area $A(x) = hl(x)$, where h is thickness in the z direction and $l(x) = \cosh^2(x/\lambda)$. (b) The total conductance divided by temperature K/T reduced by the zero-temperature universal value $\pi^2 k_B^2/3h$. The solid, dashed, dotted, and dashed-dotted curves correspond to $d_1 = d_2 = 50$ nm; $d_1 = 60$, $\lambda = 5021.6$ nm; $d_1 = 200$, $\lambda = 1653$ nm; and $d_1 = 2000$, $\lambda = 860$ nm, respectively. Here, the $d_2 = 50$, $a = 2176.9$, and $h = 50$ nm. (c) and (d) correspond to the thermal conductance for the lowest six types of vibrational modes divided by temperature K/T reduced by the zero-temperature universal value $\pi^2 k_B^2/3h$. The solid, dashed, dotted, and dashed-dotted in (c) and (d) correspond to dilatational mode, torsional mode, and two flexural modes in z and y direction, respectively. The solid and dashed curves in inserted figure in (c) and (d) correspond to two shear modes in z and y directions, respectively. The structure parameters in (c) and (d) are $d_1 = 2000$, $\lambda = 860$ nm; $d_1 = 60$, $\lambda = 5021.6$ nm, respectively. Here, $d_2 = 50$, $a = 2176.9$, and $h = 50$ nm. Reprinted with permission from Ref. [113]. Copyright (2010) by American Physical Society.

From the prospective of informatics, the heat is destructive for information memory and transport. However, the emergence of phononics make the people understand that the heat can be regarded as the information or signal. Since then, there are many novel mechanisms of thermal transport were observed in experiment and theoretical calculation, such as the thermal rectification, phonon resonance, negative thermal differential resistance, thermoelectric, and so on. The analysis of these different mechanism will be conducive to further improve the performance of nanoscale function devices.

The electron diode and spin filter device has been widely researched by theory and experiment,[115–120] as same as the electron diode, by coupling two different materials we can construct a heterojunction to form the asymmetry of heat current when the temperature difference is inverted. The first model to open the possibility of building the thermal rectifier[121] is proposed by Terraneo in 2002. Since then, the application of thermal rectification effects, such as thermal logic gates,[4] thermal transistor,[122] and thermal memory,[123] have been widely studied in theory. The first solid-state thermal rectifier experimentally also realized by using the asymmetrically mass-loaded carbon and boron nitride nanotubes.[124] In short, finding the way to control the heat transport and thermal rectification has been become an important issue for the designing of thermal devices. However, the origin of thermal rectification effect is not one-fold. Such as the interface,[125] grain boundary,[126] defect and doping,[127] mass and structure graded,[128–132] each of these can influence the thermal rectification ratio.

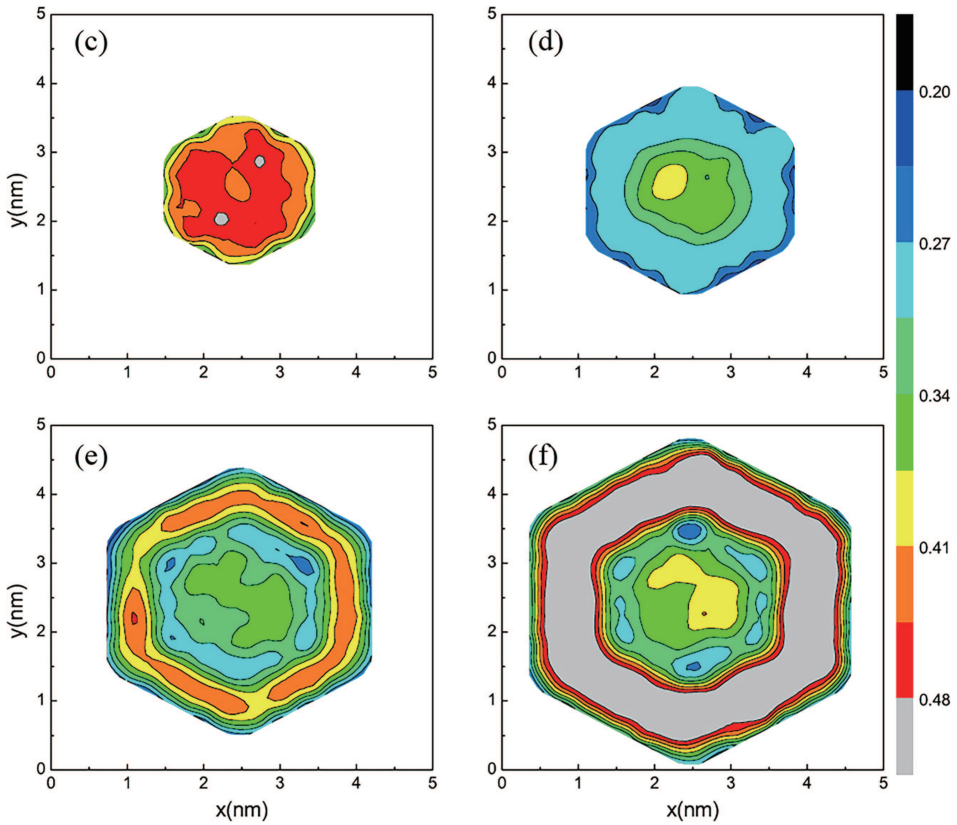


Fig. 5. (color online) (a) Cross-sectional view of GaAs/InAs (zinc blend) and InAs/GaAs (wurtzite) core-shell nanowire. The As, In, and Ga atoms are identified by black, blue, and orange, respectively. (b) Time-averaged temperature profile of the InAs/GaAs core-shell nanowire. (c)–(f) Distribution of heat flux in the cross section of InAs/GaAs core-shell nanowire. (c) is for pure InAs nanowire. (e), (f) are for InAs/GaAs core-shell nanowire with shell thickness of 0.43 nm, 0.86 nm, and 1.29 nm, respectively. Reprinted with permission from Ref. [133]. Copyright (2013) by AIP Publishing LLC.

Recently, an important mechanism to better control the heat flux in nanoscale structure was proposed by Liu *et al.*[133] They demonstrated that the core-shell nanowires have great potential to serve as a heat cable to control the channel of thermal transport. As shown in Fig. 5, in simple terms, by controlling the thickness of the cladding layers, we can effectively tune the group velocity of phonons in the nanostructure and further reengineering the phonon dispersion relations so as to obtain more excellent thermal property in nano-device. The heat flux distribution can be flexible tuned by different shell thickness and core-shell materials. In addition, this mechanism was also proved to be strongly enhancing the thermoelectric energy conversion efficiency.[134]

Accordingly, a more efficient mechanism to enhance thermal rectification ratio[135] was further examined by MD simulations. As shown in Fig. 6, the great temperature fluctuation[136] can be observed in an asymmetric graded nanowires. This phenomenon means that there are periodical nodes and antinodes formed in the entire system so as to suppressing the heat flux along the heat transport direction. These results show that the standing wave which exists in the graded nanowires can be serve as a powerful mechanism to enhance the thermal rectification effect, and serve as a fundamental mechanism for the relevant thermal transport problem. From the perspective of theory, the standing wave will be formed when the length of the nanowire and the wavelength of the thermally induced lattice wave satisfy the following re-

lationship:

$$L = n\left(\frac{\lambda}{2}\right), \quad n \subset N. \tag{42}$$

Considering the basic formula for calculating the wavelength and the determining factors of the wave velocity

$$\lambda = \frac{v}{f}, \quad v = \sqrt{\frac{F}{\rho_l}}, \tag{43}$$

where F and ρ_l denote the tension and mass density of the system. From these equations, we can easily determine that both of the different mechanical properties and the unequal vibration frequency of different materials contribute to the inequality of the wavelength. This indicates that the resonance state can be flexibly controlled by changing the length of the graded nanowires.

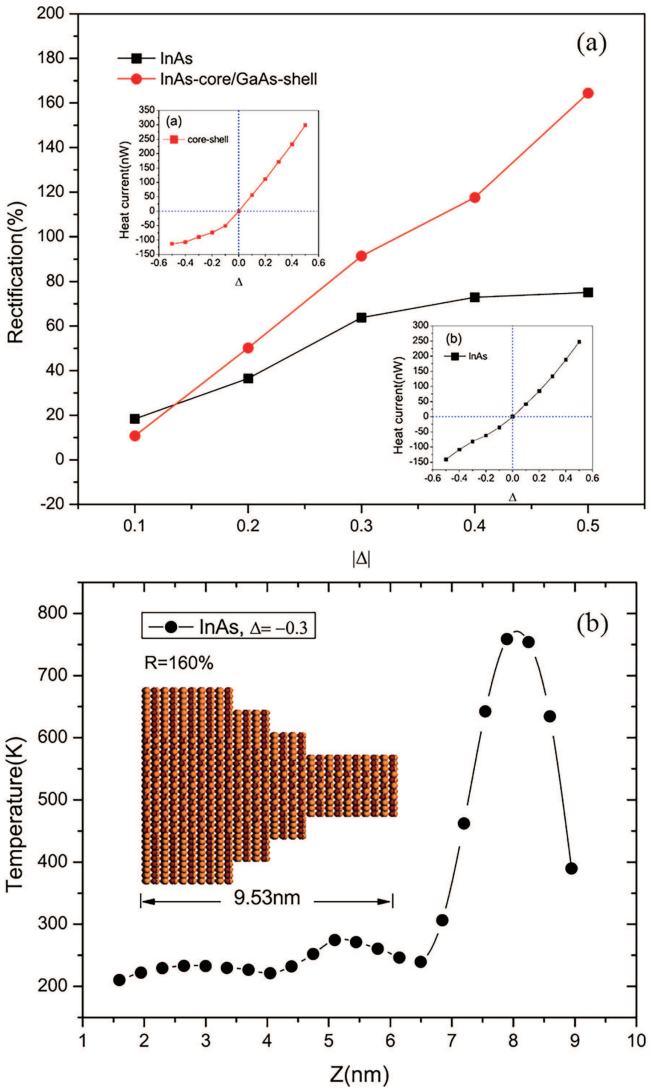


Fig. 6. (color online) (a) Thermal rectification ration of the two kinds of graded nanowire. Heat current versus temperature difference Δ is also given in the insets. (b) Structure and temperature profile of a pure InAs nanowire with wider steps, $\Delta = -0.3$. The As and In atoms are identified by brown and orange, respectively. Reprinted with permission from Ref. [135]. Copyright (2014) by AIP Publishing LLC.

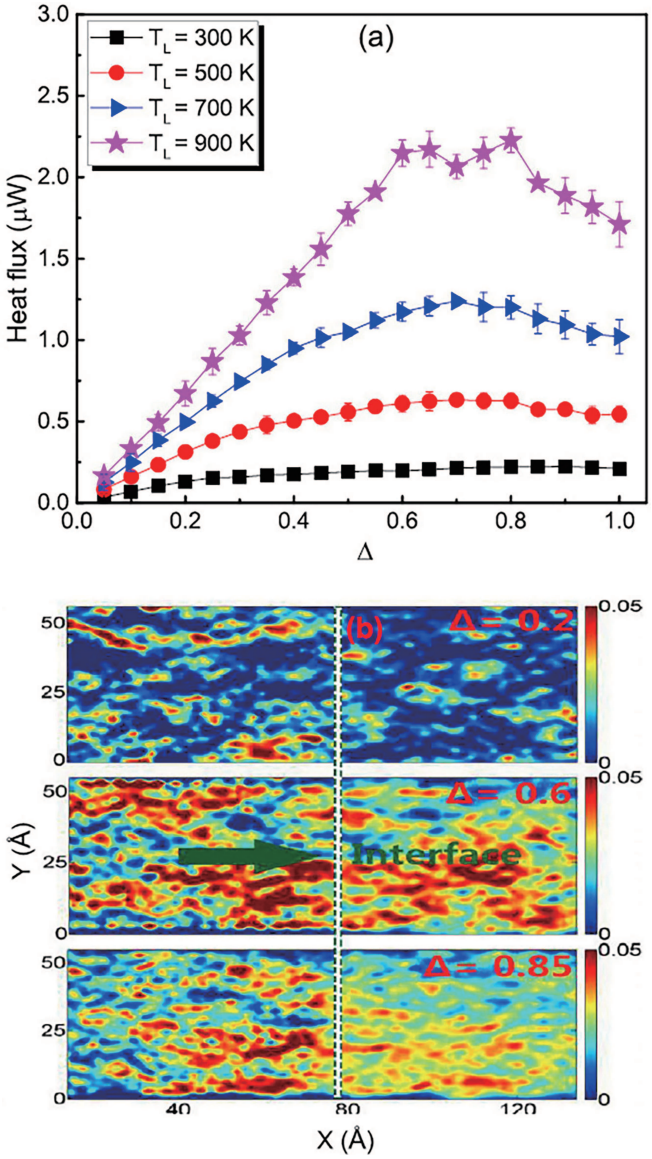


Fig. 7. (color online) (a) Effect of temperature parameter T_L on the nonlinear thermal transport. (b) Typical contour of local atomic heat flux under different Δ. Here, $T_L = 700$ K. Reprinted with permission from Ref. [138]. Copyright (2017) by AIP Publishing LLC.

The success of thermal rectifier and heat cable suggests that the heat flux can be manipulated as the signals. Most applications of thermal devices are relevant to heat conduction in the nonlinear regime. Controlling the heat flux plays a vital role in the operation of these devices. As shown in Fig. 7, there is a phenomenon similar with thermal rectification which is named negative differential thermal resistance (NDTR).[122,137,138] The NDTR can be observed at the condition of huge temperature gradient in graphene/h-BN heterostructure, which is caused by the mismatch of lateral vibration mode in graphene and h-BN domain. More interestingly, the nonlinearly thermal transport process only occur on the condition of the heat flux direction is graphene to h-BN. These results indicate that we can control the intensity of NDTR by tuning the temperature and edge size of this system. The thermal diodes and triodes, which are based on these mechanism

as discussed in above, allowing us to manipulate the heat current just like the electric current.

4. Thermoelectric property in nanoscale structures

Besides the management and manipulation of thermal energy, with the growing energy shortages, looking for a new energy of environment protection and pollution-free has been received considerable attention in recent years. Thermoelectric materials can generate electricity directly from waste heat, and thus provide a solution to these problems. It plays an important role in new energy resources field. The energy conversion efficiency of thermoelectric materials is determined by the thermoelectric figure of merit (ZT). It is defined as follows:

$$\mathrm{ZT} = \frac{\sigma S^2 T}{\kappa_{\mathrm{el}} + \kappa_{\mathrm{ph}}}, \tag{44}$$

where σ is the electronic conductance, S is the Seebeck coefficient, T is temperature, κ_{el} and κ_{ph} is the electronic and phonon thermal conductivity, respectively. From Eq. (44), we can simply see that the high ZT required the minimized thermal conductivity and maximum power factor σS^2. However, the enhancement of ZT is not a simple process. The Widermann-Franz laws[139] found that the electronic thermal conductivity κ_{el} and electrical conductance have a positive correlation with each other. The coupling relationship of these parameters can be described as follows:[140]

$$S = \frac{8\pi^2 k_{\mathrm{B}}^2}{3eh^2} m^* T \left(\frac{\pi}{3n}\right)^{2/3}, \tag{45}$$

$$\sigma = ne\mu = \frac{n\mathrm{e}^2\tau}{m^*}, \tag{46}$$

$$\kappa_{\mathrm{el}} + \kappa_{\mathrm{ph}} = L\sigma T + \kappa_{\mathrm{ph}}, \tag{47}$$

where n is the carrier concentration, τ and m^* is the density of states effective mass and relaxation time, respectively, L is the Lorenz number. In general, the power factor is influenced by scattering rate, energy state density, carrier mobility, and fermi level. However, the former three property was determined by the intrinsic property of materials, so that, from the above relationship we can see that there are two better pathways to enhance the performance of thermoelectricity in present, i.e., band structure engineering and reduction of lattice thermal conductivity. On one hand, through the careful and effective adjustment of bandstructure,[141,142] we can obtain higher effective mass of electron and more valley structure in band structure so as to enhance the ZT value. On the other hand, the reduction of lattice thermal conductivity or the intrinsic ultra-low thermal conductivity materials can also improve overall performance of the thermoelectric energy conversion. The lower phonon thermal conductivity means the higher temperature difference will be induced in both ends of system so as to enhance the ZT in a constant temperature.

On the one hand, there are various ways to enhance thermoelectric energy conversion efficient of inorganic crystals, such as defect[143–145] and doping,[146–148] core-shell structure,[149–151] superlattice,[152,153] branch structure,[154,155] strain[156,157] and electric field engineering,[158] phonon-drag effect,[159] and so on, which are widely studied in experiment and theoretical simulation.

For the thermoelectric performance regulation, the defect and doping plays vital roles in reduction of phonon thermal conductivity, which can be obviously suppress the phonon vibration density of states in the entire frequency range, As is shown in Fig. 8. Compared with the case of without defect, the phonon thermal conductivity is only around one fourth of its in the condition of vacancy defect existence. Both of the low and high frequency phonon modes are remarkable suppressed by vacancy defect. Moreover, the power factor have also not affected by vacancy defect in middle and high temperature region so that the ZT increases with increasing temperature obviously.

Another efficient way to obtain high ZT is superlattice structure, as shown in Fig. 9, Chen *et al.*[152] demonstrated that with the increase/decrease in period length, there will exist a minimum thermal conductivity in superlattice system. The temperature behavior presents a wave-like characterize, which indicates that the phonon transport will experience transition process from coherent to incoherent when the periodic length L_{p} tends to be a specific length. A follow-up work also shows that the ZT value of similar structure could be as large as 2.7 at 300 K,[160] which indicates that these structures have great potential to serve as powerful thermoelectric energy conversion device.

While as for the strain engineering, we can see that, the phonon frequency will redshift with the strain loaded, as show in Fig. 10, so as to hold down the thermal conductivity of entire system. These methods discussed above can be combined with each other to enhance the performance of thermoelectric materials more efficiently. In short, the underlying physical mechanism for thermoelectric, such as the correctness of the Widermann–Franz laws, is still unclear in low dimensional and extreme physical environment. From the theoretical standpoint, the decoupling of each parameter of ZT also a direction with challenges and potential, which can be further enhance the performance of thermoelectric energy conversion efficient.

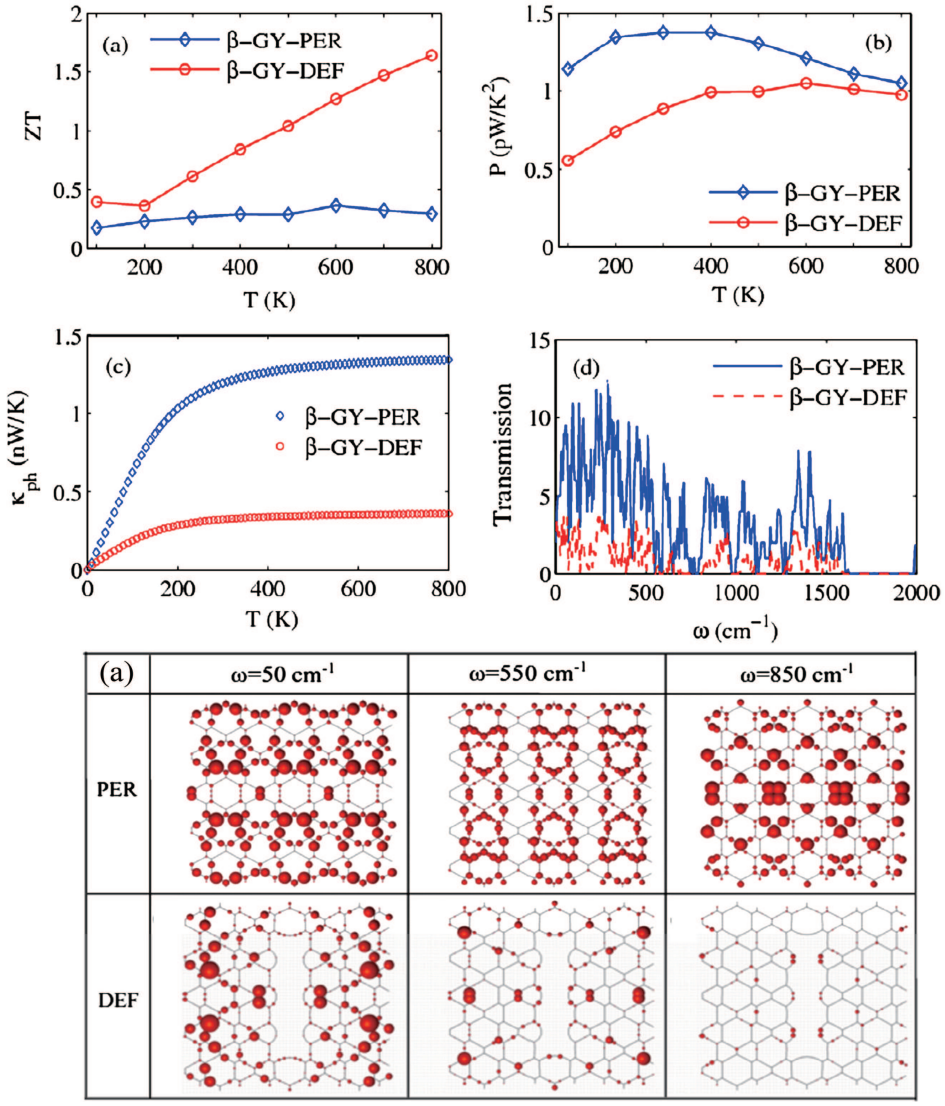


Fig. 8. (color online) (a), (b) The ZT value and power factor of perfect and defect β-graphyne; (c) phonon thermal conductivity with defect and without defect; (d) phonon transmission coefficient with defect and without defect; (e) localized phonon density of state for pristine and defective β-graphyne at the different typical frequencies. Reprinted with the permission from Ref. [145]. Copyright (2017) by Elsevier.

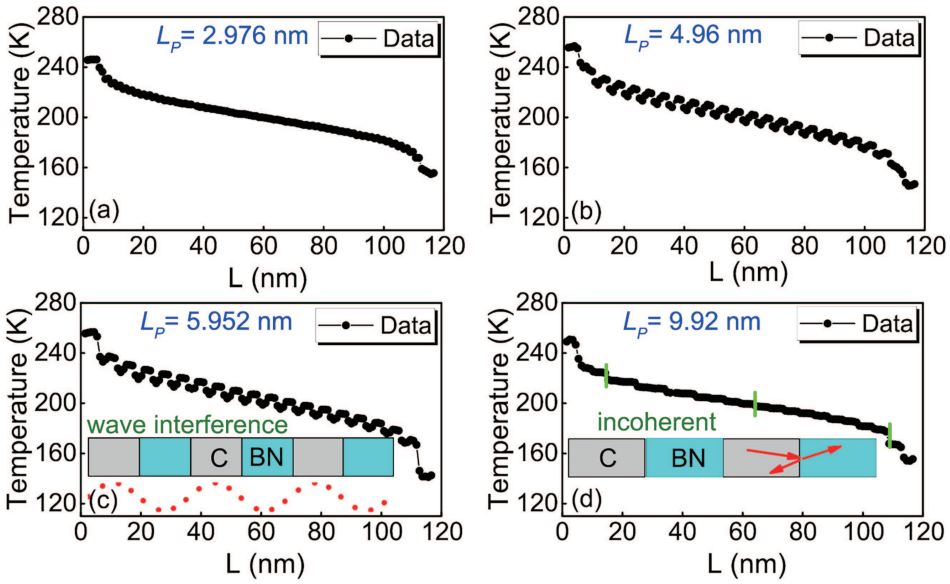


Fig. 9. (color online) Temperature distribution of single-layer BNC with different periodic length L_p at 200 K. Reprinted with the permission from Ref. [152]. Copyright (2017) by AIP Publishing LLC.

Besides the bulk materials, with the progressing of molecular synthetic technique, the organic molecular system[161–168] has also been paid more attention in recent years. The molecular junction[169–173] and molecular crystals,[174] and so on were both expected to serve as the powerful thermoelectric materials. The electrode and molecule are coupling with each other,[175] which is dynamics coupling between transmitted electrons and molecular vibration that can strongly affect the transmission process of electron so that we have to consider the electron–phonon coupling effect in molecule devices. Without considering electron–phonon coupling effect, based on nonequilibrium Green's function method, Cao *et al.*[176] confirmed that compared with the perfect graphene nanoribbon, the single molecular will dramatically enhance the scattering rate of phonon so as to greatly reduces the thermal conductivity of both acoustic and optical phonon, as shown in Figs. 11(a) and 11(b).

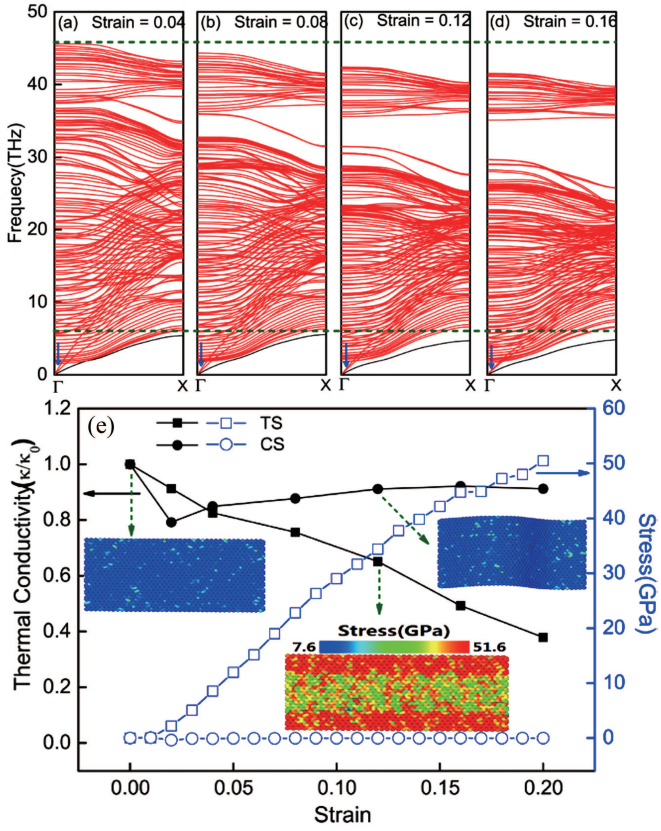


Fig. 10. (color online) (a)–(d) Phonon dispersion relations with strain of 0.04, 0.08, 0.12, 0.16 at 300 K. (e) Normalized thermal conductivity and stress (κ/κ_0 of h-BN/graphene heterostructure as a function of strain, where the strain along the x direction. The stress distribution is given in insert. Reprinted with the permission from Ref. [156]. Copyright (2017) by IOP Publishing.

Furthermore, an interesting phenomenon will be founded when we take the electron–phonon interaction into account in molecule system, that is, the electric current will obviously enhanced by electron–phonon coupling,[177–179] as shown in Figs. 10(d)–10(f). It is easy to see that both of the electric and magnetic properties was hugely influenced by the propagation of phonon. From the perspective of the weight of specific phonon mode in phonon dispersion relations, the electron-phonon coupling effect in the dynamical area of graphene device originates mainly from the optical phonon. And the spin current with and without considering the electron–phonon coupling effect makes huge different. Obviously, the spin filter phenomenon was destructed by lattice vibration. As shown in Figs. 10(a)–10(c), a recent study also confirm this phenomenon by combining MD and NEGF method.[180] These results mean that the spin filter phenomenon may not be observing in room temperature unless the phonon vibration was suppressed by another physical or chemical method. Almost simultaneously, the experiment is confirmed the room temperature spin filter by using the Ni/graphene/Fe van der waals heterostructure,[181] which is a direct evidence for the significance of electron–phonon coupling effect in nano-device. However, the present theory for electron–phonon coupling is just considering the interaction of ballistic phonon and electrons,[182–185] it is still insufficient for reconstruct the real physical process. This in turn requires further understanding of electron-phonon interaction in real system. It may promote greatly the progress of thermoelectricity and electric devices.

On the other hand, the parameters coupling relationship of ZT has always plagued us so that the energy conversion efficiency is difficult to improve. Except the traditional thermoelectric effect, the piezoelectric effect and triboelectric effect also have great potential to convert disorder energy into usable energy. Since the realization of piezoelectric in Zinc Oxide nanowires[186] in 2006, piezoelectricity have been a real hotspot in recent years. Various nanogenertors based on different materials have been developed,[187–189] and the application of these nanogenertors has covered electronics powering, signal sensing and so on. However, the energy source of piezoelectricity is usually irregular ambient natural energy like wind or manually provided mechanical energies, and consequently, either the output electric potential is aperiodic or the energy source is not the basic energy like heat in our nature. The advantage of thermoelectric can directly convert heat energy into electricity, but the output is limited to direct current and the difficulty in increasing the efficiency is widely known.

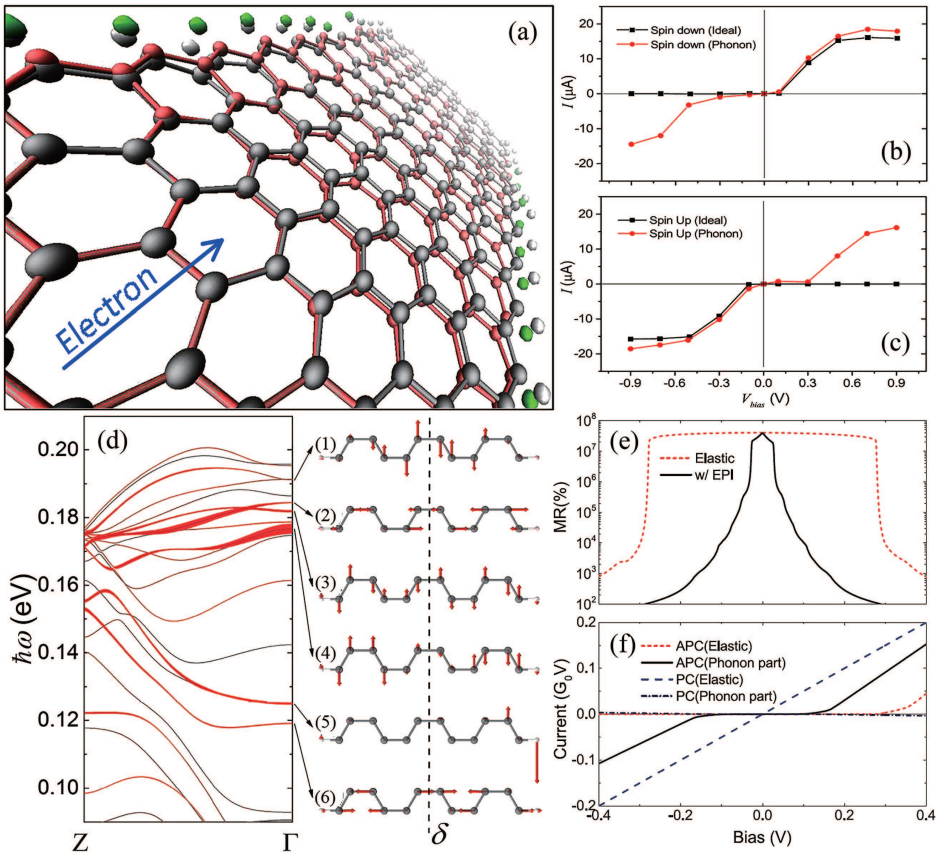


Fig. 11. (color online) (a) Structure deformation of 8-ZGNR induced by temperature effect. The C and H atoms at two different moments are represented by gray and silver, and red and green, respectively. (b) and (c) The spin I–V curve of the ideal 8-ZGNR and 8-ZGNR with phonon effect. (d) The phonon band structure of infinite GNRs. The widths of the red bands are proportional to the weight function of electron-phonon interaction, where the (1-6) represent the phonon modes at the Γ point of the six most effective bands. The dashed line shows the structural symmetric mirror plane δ through the center of GNR. (e) The magnetoresistances (MR) of ferromagnetic 6-ZGNR with (solid line) and without (dashed line) consideration of electron-phonon interaction at 4.2 K. (f) The spin up current of the elastic $I_{\rm el}$ and phonon-influenced $I_{\rm ph}$ parts in parallel and antiparallel configurations at 4.2 K. Reprinted Figs. 10(a)–10(c) and 10(d)–10(f) with permissions from Ref. [177] and Ref. [180], respectively. Copyright (2017) by AIP Publishing LLC and copyright (2016) by IOP Publishing.

Encouragingly, utilizing the molecular dynamics simulation, Liu *et al.*[190] predicted a novel mechanism for thermoelectric energy conversion based on the combination of lattice dynamic and piezoelectric effect. As is known, the lattice wave can be approximately regarded as the harmonic vibration so that the amplitude of the vibration can be easily estimated by the following classical equation:

$$E = \frac{1}{2} m A^2 \omega^2, \tag{48}$$

where the m is the mass of atom, ω is vibration frequency. Considering the quantized of phonon energy, which is given by

$$E_j(T) = \frac{1}{2}\hbar\omega_j + \frac{\hbar\omega_j}{\exp\left(\dfrac{\hbar\omega_j}{k_{\rm B}T}\right) - 1}. \tag{49}$$

We can approximately obtaining the amplitude of lattice wave by combining the Eqs. (48) and (49) under the harmonic approximation. Interestingly, the result suggests that the vibration amplitude in nanoscale will be more larger than macroscopic materials. However, the vibration amplitude of nanowires in constant temperature is still insufficient to applied on piezoelectric materials. To enlarge the deflection degree of this phenomenon, we introduce a temperature gradient along the nanowires into all system so that the periodic deflect can be obtained by direct heating the local few layers atom of GaN nanowire. The maximum bending radius as large as 9 nm and 5 nm in ZnO and GaN nanowire respectively. These values has been many times larger than the amplitude of the lattice wave excited by unitary heating. And the obvious piezoelectric potential, which is reached 0.34 V, can be observed in this condition. This energy conversion process provide another way to convert the thermal energy to electric energy rather than dependent on Seebeck effect. Moreover, the realization of this mechanism is independent of the materials. We can thus realize this mechanism not only in GaN and ZnO nanowires, but also in other III–V semiconductor nanowires and II–VI semiconductor nanowires, and so on.

5. Conclusion

We present a brief overview of the different theoretical model in nanoscale thermal transport field, and a serial of nov-

elty phenomena were predicted by these model. At first, we introduced several kinds of theoretical method and the application range of different theories from the ballistic to diffusion transport. At present, the theoretical research of heat transport still lacking a standard model for different systems so that the choice of method is so important, which has a direct impact on the correctness of the results. The introduction and comparison of different theoretical methods aim to provide better choice and guidance to study the heat transport properties in different system.

Based on these theoretical models, we present several efficient ways to manipulate the heat flux. And the various novel thermal transport mechanism in nanoscale structure were predict by theoretical simulation, such as the various defect effect, standing waves, negative differential thermal resistance, the destructive of spin filter by phonon. These studies are mainly focus on the regulation of electron and phonon properties. Moreover, we designed a series of approaches to remarkable enhance the thermoelectric performance in nanoscale structure. For the follow-up researches, these discovers could be provide a guideline for design and theory research on microelectronic device so that to further promote the application of thermal and thermoelectric energy conversion devices.

References

[1] Zhao L D, Lo S H, Zhang Y S, Sun H, Tan G J, Uher C, Wolverton C, Dravid V P and Kanatzidis M G 2014 *Nature* **508** 373
[2] Xu Y, Gan Z X and Zhang S C 2014 *Phys. Rev. Lett.* **112** 226801
[3] Li B W, Wang L and Casati G 2004 *Phys. Rev. Lett.* **93** 184301
[4] Wang L and Li B W 2007 *Phys. Rev. Lett.* **99** 177208
[5] Liu Y Z, Xu Y and Duan W H 2017 *National Science Review* **00** 1–3
[6] Zhang L F, Ren J, Wang J S and Li B W 2010 *Phys. Rev. Lett.* **105** 225901
[7] Liu Y Z, Y Xu, Zhang S C and Duan W H 2017 *Phys. Rev. B* **96** 064106
[8] Sugii K, Shimozawa M, Watanabe D, Suzuki Y, Halim Y, Kimata M, Matsumoto Y, Nakatsuji S and Yamashita M 2017 *Phys. Rev. Lett.* **118** 145902
[9] Liu Y, Lian C S, Li Y, Xu Y and Duan W H 2017 *Phys. Rev. Lett.* **119** 255901
[10] Cho A Y and Aathur J R 1975 *Prog. Solid State Ch.* **10** 157–191
[11] Hampden-Smith M J and Kodas T T 1995 *Chem. Vapor Depos.* **1** 8
[12] Narducci D 2011 *Appl. Phys. Lett.* **99** 102104
[13] Tan G, Zhao L D and Kanatzidis M G 2016 *Chem. Rev.* **116** 12123
[14] Pengv J B, Zhang G and Li B W 2015 *Appl. Phys. Lett.* **107** 133108
[15] Yap H H and Wang J S 2015 *Phys. Rev. Lett.* **95** 012126
[16] Li N B, Ren J, Wang L, Zhang G, Hänggi P and Li B W 2012 *Rev. Modern Phys.* **84** 1045
[17] Novoselov K S, Geim A K, Morozov S V, Jiang D, Zhang Y, Dubonos S V, Grigorieva I V and Firsov A A 2004 *Science* **306** 666
[18] Jiang Z, Liu Z, Li Y and Duan W 2017 *Phys. Rev. Lett.* **118** 266401
[19] Liu H, Neal A T, Zhu Z, Luo Z, Xu X, Tománek D and Ye P D 2014 *ACS nano* **8** 4033
[20] Hou J G, Wang B, Yang J, Wang X R, Wang H Q, Zhu Q and Xiao X 2001 *Phys. Rev. Lett.* **86** 5321
[21] Li N, Li B and Flach S 2010 *Phys. Rev. Lett.* **105** 054102
[22] Liu S, Hänggi P, Li N, Ren J and Li B 2014 *Phys. Rev. Lett.* **112** 040601
[23] Chen K Q, Wang X H and Gu B Y 2000 *Phys. Rev. B* **61** 12075
[24] Li W X, Q Chen K, Duan W H, Wu J and Gu B L 2003 *J. Phys. D: Appl. Phys.* **36** 3027
[25] Jiang J W, Wang B S and Wang J S 2011 *Phys. Rev. B* **83** 235432
[26] Wang J S, Wang J and Zeng N 2006 *Phys. Rev. B* **74** 033408
[27] Cepellotti A and Marzari N 2017 *Nano Lett.* **17** 4675
[28] Leivo M M and Pekola J P 1998 *Appl. Phys. Lett.* **72** 1305
[29] Holmes W, Gildemeister J M, Richards P L and Kotsubo V 1998 *Appl. Phys. Lett.* **72** 2250
[30] Li W X, Liu T Y and Liu C L 2006 *Appl. Phys. Lett.* **89** 163104
[31] Peng X F, Wang X J, Chen L Q and Chen K Q 2012 *Euro. Phys. Lett.* **98** 56001
[32] Santamore D H and Cross M C 2001 *Phys. Rev. Lett.* **87** 115502
[33] Chen K Q, Li W X, Duan W H, Shuai Z and Gu B L 2005 *Phys. Rev. B* **72** 045422
[34] Tang L M, Wang L L, Chen K Q, Huang W Q and Zou B S 2006 *Appl. Phys. Lett.* **88** 163505
[35] Peng X F, Chen K Q and Zhang B S 2007 *Appl. Phys. Lett.* **90** 193502
[36] Chen K Q, Wang X H and Gu B Y 2000 *Phys. Rev. B* **62** 9919
[37] Chen K Q, Duan W H, Wu J, Gu B L and Gu B Y 2002 *J. Phys.: Codens. Matter* **14** 13761
[38] Li W X, Chen K Q, Duan W H, Wu J and Gu B L 2003 *Phys. Lett. A* **308** 285
[39] Mingo N 2006 *Phys. Rev. B* **74** 125402
[40] Xu Y, Wang J S, Duan W H, Gu B L and Li B W 2008 *Phys. Rev. B* **78** 224303
[41] Lü J T and Wang J S 2007 *Phys. Rev. B* **76** 165418
[42] Segal D, Nitzan A and Hänggi P 2003 *J. Chem. Phys.* **119** 6840
[43] Mingo N and Liu Y 2003 *Phys. Rev. B* **68** 245406
[44] Galperin M, Nitzan A and Ratner M A 2007 *Phys. Rev. B* **75** 155312
[45] Wang J S, Zeng N, Wang J and Gan C K 2007 *Phys. Rev. E* **75** 061128
[46] Chen X B and Duan W H 2015 *Acta. Phys. Sin.* **18** 186302 (in Chinese)
[47] Peng X F, Wang X J, Gong Z Q and Chen K Q 2011 *Appl. Phys. Lett.* **99** 233105
[48] Chen G 2001 *Phys. Rev. Lett.* **86** 2297
[49] Chen J, Zhang G and Li B W 2009 *Appl. Phys. Lett.* **95** 073117
[50] Wang J S and Zhang L F 2009 *Phys. Rev. B* **80** 012301
[51] Hu L, Zhang L, Hu M, Wang J S, Li B W and Keblinski P 2010 *Phys. Rev. B* **81** 235427
[52] Guo Z X, Ding J W and Gong X G 2012 *Phys. Rev. B* **85** 235429
[53] Zhang H S, Guo Z X, Gong X G and Cao J X 2012 *J. Appl. Phys.* **112** 123508
[54] Ye X, Sun D Y and Gong X G 2005 *Phys. Rev. B* **72** 035454
[55] Gu M X, Sun C Q, Chen Z, Au Yeung T C, Li S, Tan C M and Nosik V 2007 *Phys. Rev. B* **75** 125403
[56] Sun C Q 2007 *Prog. Solid State Ch.* **35** 1–159
[57] Ye X, Sun D Y and Gong X G 2007 *Phys. Rev. B* **75** 073406
[58] Sun C Q 2009 *Prog. Mater. Sci.* **54** 179
[59] Guo N G, Zhou Z F, Huang Y L, Yang X X, Jiang R, Maa Z S and Sun C Q 2013 *Chem. Phys. Lett.* **585** 167
[60] Alexeev D, Chen J, Walther J H, Giapis K P, Angelikopoulos P and Koumoutsakos P 2015 *Nano Lett.* **15** 5744
[61] Sun D Y, Liu J W, Gong X G and Liu Z F 2007 *Phys. Rev. B* **75** 075424
[62] Chen J, Walther J H and Koumoutsakos P 2015 *Adv. Func. Mat.* **25** 7539
[63] Gong X G 1993 *Phys. Rev. B* **47** 2329
[64] Sun D Y and Gong X G 1996 *Phys. Rev. B* **54** 17051
[65] Wei L, Xu Z C, Zheng D Q, Zhang W and Zhong W R 2015 *Chin. Phys. Lett.* **32** 076501
[66] Yu C X, Zhang G, Peng L M, Duan W H and Zhang Y W 2014 *Appl. Phys. Lett.* **105** 023903
[67] Nosé S 1984 *J. Chem. Phys.* **81** 511
[68] Hoover W G 1985 *Phys. Rev. A* **31** 1695
[69] Soddemann T, Dünweg B and Kremer K 2003 *Phys. Rev. E* **68** 046702
[70] Evans D J 1985 *Phys. Rev. A* **32** 2923
[71] Takesue S 1988 *Phys. Rev. Lett.* **64** 252
[72] Turney J E, McGaughey A J H and Amon C H 2009 *Phys. Rev. B* **79** 224305
[73] Wang J S 2007 *Phys. Rev. Lett.* **99** 160601
[74] Lü J T and Wang J S 2008 *J. Phys.: Condens. Matter* **21** 025503
[75] Feng T L and Ruan X L 2016 *Phys. Rev. B* **93** 045202
[76] FengT L, Lindsay L and Ruan X L 2017 *Phys. Rev. B* **96** 161201
[77] Shen Y L, Xie G F, Wei X L, Zhang K W, Tang M H, Zhong J X, Zhang G and Zhang Y W 2014 *J. Appl. Phys.* **115** 063507

[78] Xie G F, Guo Y, Wei X L, Zhang K W, Sun L Z, Zhong J X, Zhang G and Zhang Y W 2014 *Appl. Phys. Lett.* **104** 233901
[79] Zhou W X and Chen K Q 2015 *Sci. Rep.* **5** 15070
[80] Sun Y J, Wang D and Shuai Z G 2008 *J. Phys. Chem. C* **121** 19080
[81] Ren H, Li Q X, Luo Y and Yang J L 2009 *Appl. Phys. Lett* **94** 173110
[82] Pan Z, Heb L, Qiu L, Korayem A H, Li G, Zhu J W, Collins F, Li D, Duan W H and Wang M C 2015 *Cement Concrete Comp.* **58** 140
[83] Ouyang T, Chen Y P, Xie Y, Stocks G M and Zhong J X 2011 *Appl. Phys. Lett.* **99** 233101
[84] Xu Y, Chen X B, Gu B L and Duan W H 2009 *Appl. Phys. Lett.* **95** 233116
[85] Guo Z X, Zhang D and Gong X G 2009 *Appl. Phys. Lett.* **95** 163103
[86] Wang J, Lian B, Zhang H J, Xu Y and Zhang S C 2013 *Phys. Rev Lett.* **111** 136801
[87] Wei X L, Wang Y C, Shen Y L, Xie G F, Xiao H P, Zhong J X and Zhang G 2014 *Appl. Phys. Lett.* **105** 103902
[88] Ouyang T, Chen Y P, Liu L M, Xie Y, Wei X L and Zhong J X 2012 *Phys. Rev. B* **85** 235436
[89] Wu X J, Dai J, Zhao Y, Zhuo Z W, Yang J L and Zeng X C 2012 *ACS Nano* **6** 8
[90] Vogt P, De Padova P, Quaresima P, Avila J, Frantzeskakis E, AsensioM C, Resta A, Ealet B and Lay G L 2012 *Phys. Rev. Lett.* **108** 155501
[91] Zhang G and Zhang Y W 2017 *Chin. Phys. B* **26** 034401
[92] Liang L H and Li B W 2006 *Phys. Rev. B* **73** 153303
[93] Hu S Q, Chen J, Yang N and Li B W 2017 *Carbon* **116** 139
[94] Li D F, Xu Y, Chen X B, Li B L and Duan W H 2014 *Appl. Phys. Lett.* **104** 143108
[95] Lan J, Wang J S, Gan C K and Chin S K 2009 *Phys. Rev. B* **79** 115401
[96] France-Lanord A, Soukiassian P, Glattli C and Wimmer E 2017 *Phys. Rev. Appl.* **7** 034030
[97] Xie Z X, Chen K Q and Duan W 2011 *J. Phys.: Codens. Matt.* **23** 315302
[98] Chen K Q, Wang X H and Gu B Y 2002 *Phys. Rev. B* **65** 153305
[99] Morooka M, Yamamoto T and Watanabe K 2008 *Phys. Rev. B* **77** 033412
[100] Peng X F and Chen K Q 2014 *Carbon* **77** 3605
[101] Xie Z X, Chen K Q and Tang L M 2011 *J. Appl. Phys.* **110** 124321
[102] Yang N, Zhang G and Li B W 2008 *Nano Lett.* **8** 276
[103] Chen X B, Xu Y, Zou X L, Gu B L and Duan W H 2013 *Phys. Rev. B* **87** 155438
[104] Wang J, Li L and Wang J S 2011 *Appl. Phys. Lett.* **99** 091905
[105] Yao Z H, Wang J S, Li B W and Liu G R 2005 *Phys. Rev. B* **71** 085417
[106] Zhu H Q, Xu Y, Gu B L and Duan W H 2012 *New J. Phys.* **14** 013053
[107] Xu Y, Chen X B, Wang J S, Gu B L and Duan W H 2010 *Phys. Rev. B* **81** 195425
[108] Yi M and Xing D 2008 *Chin. Phys. Lett.* **31** 080501
[109] Li B W and Wang J 2003 *Phys. Rev. Lett.* **91** 044301
[110] Lü J T, Christensen R B, Wang J S, Hedegård P and Brandbyge M 2014 *Phys. Rev. Lett.* **114** 096801
[111] Li W X, Chen K Q, Duan W, Wu J and Gu B L 2004 *Appl. Phys. Lett.* **85** 822
[112] Zhang L F, Yan Y H, Wu C Q, Wang J S and Li B W 2009 *Phys. Rev. B* **80** 172301
[113] Peng X F, Chen K Q, Wan Q, Zou B S and Duan W H 2010 *Phys. Rev. B* **81** 195317
[114] Li W X, Chen K Q, Duan W H, Wu J and Gu B L 2004 *J. Phys.: Condens. Matter* **16** 5049
[115] Jiang B, Zhou Y H, Chen C Y and Chen K Q 2015 *Org. Electron* **23** 133
[116] Zeng J and Chen K Q 2014 *Appl. Phys. Lett.* **104** 033104
[117] Zhou Y H, Tan S H and Chen K Q 2014 *Org. Electron* **15** 3392
[118] Peng J, Zhou Y H and Chen K Q 2014 *Org. Electron* **27** 137
[119] Ling Y C, Ning F, Zhou Y H and Chen K Q 2015 *Org. Electron* **19** 92
[120] Tan C M, Zhou Y H, Chen C Y, Yu J F and Chen K Q 2016 *Org. Electron* **28** 244
[121] Terraneo M, Peyrard M and Casati G 2002 *Phys. Rev. Lett.* **88** 094302
[122] Li B W, Wang L and Casati G 2006 *Appl. Phys. Lett.* **88** 143501
[123] Wang L and Li B W 2008 *Phys. Rev. Lett.* **101** 267203
[124] Chang C W, Okawa D, Majumdar A and Zettl A 2006 *Science* **314** 5802
[125] Lan J H and Li B W 2006 *Phys. Rev. B* **74** 214305
[126] Cao H Y, Xiang H J and Gong X G 2012 *Solid State Commun.* **152** 1807
[127] Wu G and Li B W 2007 *Phys. Rev. B* **76** 085424
[128] Hu M, Keblinski P and Li B W 2008 *Appl. Phys. Lett.* **92** 211908
[129] Ouyang T, Chen Y P, Xie Y, Wei X L, Yang K K, Yang P and Zhong J X 2010 *Phys. Rev. B* **82** 245403
[130] Xie Z X, Li K M, Tang L M, Pan C N and Chen K Q 2012 *Appl. Phys. Lett.* **100** 183110
[131] Yang N, Zhang G and Li B W 2008 *Appl. Phys. Lett.* **93** 243111
[132] Yang N, Zhang G and Li B W 2009 *Appl. Phys. Lett.* **95** 033107
[133] Liu Y Y, Zhou W X, Tang L M and Chen K Q 2013 *Appl. Phys. Lett.* **103** 263118
[134] Zhou W X and Chen K Q 2013 *Sci. Rep.* **4** 7150
[135] Liu Y Y, Zhou W X, Tang L M and Chen K Q 2014 *Appl. Phys. Lett.* **105** 203111
[136] Xiong S Y, Sääskilahti K, Kosevich Y A, Han H X, Donadio D and Volz S 2016 *Phys. Rev. Lett.* **117** 025503
[137] Chen X K, Xie Z X, Zhou W X, Tang L M and Chen K Q 2016 *Carbon* **100** 492
[138] Chen X K, Liu J, Peng Z H, Du D and Chen K Q 2017 *Appl. Phys. Lett.* **110** 091907
[139] Graf M J, Yip S K, Sauls J A and Rainer D 1993 *Phys. Rev. B* **53** 15147
[140] Zhang X and Zhao L D 2015 *J. Materiomics* **1** 92
[141] Xiang H J, Huang B, Kan E J, Wei S H and Gong X G 2013 *Phys. Rev. Lett.* **110** 118702
[142] Huang Z Y, He C Y, Qi X, Yang H, Liu W L, Wei X L, Peng X Y and Zhong J X 2014 *J. Phys. D: Appl. Phys.* **47** 075301
[143] Huang H Q, Xu Y, Zou X L, Wu J and Duan W 2013 *Phys. Rev. B* **87** 205415
[144] Ni X X, Liang G C, Wang J S and Li B W 2009 *Appl. Phys. Lett.* **95** 192114
[145] Zhou W X and Chen K Q 2011 *Carbon* **85** 24
[146] Chen J, Zhang G and Li B W 2010 *Nano Lett.* **10** 3978
[147] Shi L H, Yao D L, Zhang G and Li B W 2010 *Appl. Phys. Lett.* **96** 173108
[148] Xie Z X, Tang L M, Pan C N, Chen Q and Chen K Q 2013 *J. Appl. Phys.* **114** 144311
[149] Chen J, Zhang G and Li B 2012 *Nano Lett.* **12** 2826–2832
[150] Xie G F, Li B H, Yang L W, Cao J X, Guo Z X, Tang M H and Zhong J X 2013 *J. Appl. Phys.* **113** 083501
[151] Zhou W X, Tan S H, Chen K Q and Hu W P 2014 *J. Appl. Phys.* **115** 124308
[152] Chen X K, Xie Z X, Zhou W X, Tang L M and Chen K Q 2016 *Appl. Phys. Lett.* **109** 023101
[153] Yang K K, Chen Y P, D'Agosta R, Xie Y, Zhong J X and Rubio A 2012 *Phys. Rev. B* **86** 045425
[154] Pan C N, Xie Z X, Tang L M and Chen K Q 2012 *Appl. Phys. Lett.* **101** 103115
[155] Xie Z X, Tang L M, Pan C N, Li K M, Chen K Q and Duan W H 2012 *Appl. Phys. Lett.* **100** 073105
[156] Chen X K, Xie Z X, Zhou W X and Chen K Q 2016 *J. Phys. D: Appl. Phys.* **49** 115301
[157] Sun L, Li Q X, Ren H, Su H B, Shi Q W and Yang J L 2008 *J. Chem. Phys.* **129** 074704
[158] Kan E J, Li Z Y, Yang J L and Hou J G 2007 *Appl. Phys. Lett.* **91** 243116
[159] Lü J T, Wang J S, Hedegård P and Brandbyge M 2016 *Phys. Rev. B* **93** 205404
[160] Ouyang Y L, Xie Y, Zhang Z W, Peng Q and Chen Y P 2016 *J. Appl. Phys.* **120** 235109
[161] Zhang Z H, Deng X Q, Tan X Q, Qiu M and Pan J B 2010 *Appl. Phys. Lett.* **97** 183105
[162] Pan J B, Zhang Z H, Ding K H, Deng X Q and Guo C 2011 *Appl. Phys. Lett.* **98** 092102
[163] Pan J B, Zhang Z H, Deng X Q, Qiu M and Guo C 2016 *Appl. Phys. Lett.* **98** 013503
[164] Zhang Z H, Guo C, Kwong D J, Li J, Deng X Q and Fan Z Q 2016 *Adv. Func. Mater.* **23** 2765

[165] Zhang Z H, Zhang J J, Kwong G, Li J, Fan Z Q, Deng X Q and Tang G P 2016 *Sci. Rep.* **3** 2575
[166] Guo J, Lü J T, Feng Y X, Chen J, Peng J B, Lin Z, Meng X Z, Wang Z C, Li X Z, Wang E G and Jiang Y 2016 *Science* **352** 321
[167] Sun Y, Ma Y, Liu Y, Lin Y, Wang Z, Wang Y, Di C, Xiao K, Chen X, Qiu W, Zhang B, Yu G, Hu W and Zhu D 2006 *Adv. Func. Mater.* **16** 426
[168] Ying H, Zhou W X, Chen K Q and Zhou G 2014 *Comp. Mater. Sci.* **82** 33
[169] Hu W, Jiang J, Nakashima H, Luo Y, Kashimura Y, Chen K Q, Shuai Z, Furukawa K, Lu W, Liu Y, Zhu D and Torimitsu K 2006 *Phys. Rev. Lett.* **96** 27801
[170] Ren J, Zhu J X, Gubernatis J E, Wang C and Li B W 2012 *Phys. Rev. B* **85** 155443
[171] Wei D C, Xie L F, Lee K K, Hu Z B, Tan S H, Chen W, Sow C H, Chen K Q, Liu Y and Wee A T S 2013 *Nat. Commun.* **4** 1374
[172] Kuang G W, Chen S Z, Wang W H, Lin T, Chen K Q, Shang X S, Liu P N and Lin N 2016 *J. Am. Chem. Soc.* **138** 11140
[173] Kuang G W, Chen S Z, Yan L H, Chen K Q, Shang X S, Liu P N and Lin N 2018 *J. Am. Chem. Soc.* **140** 570
[174] Mi X Y, Yu X X, Yao K L, Huang X M, Yang N and Lü J T 2015 *Nano Lett.* **15** 5229
[175] Galperin M, Ratner M A and Nitzan A 2007 *J. Phys.: Condens. Matter* **19** 103201
[176] Cao X H, Zhou W X, Chen C Y, Tang C Y, Long M Q and Chen K Q 2017 *Sci. Rep.* **7** 10842
[177] Li B L and Chen K Q 2017 *J. Phys.: Condens. Matter* **29** 075301
[178] Li B L and Chen K Q 2017 *Carbon* **119** 548
[179] Li B L, Feng Y X and Chen K Q 2018 *Org. Electron.* **54** 89
[180] Liu Y Y, Li B L, Chen S Z, Jiang X W and Chen K Q 2017 *Appl. Phys. Lett.* **111** 133107
[181] Cobas E D, van't Erve O M J, Cheng S F, Culbertson J C, Jernigan G G, Bussman K and Jonker B T 2016 *ACS Nano* **10** 10357
[182] Lü J T and Wang J S 2008 *Phys. Rev. B* **78** 235436
[183] Lü J T, Christensen R B, Foti G, Frederiksen T, Gunst T and Brandbyge M 2014 *Phys. Rev. B* **89** 081405
[184] Peng X F, Zhou X, Jiang X T, Gao R B, Tan S H and Chen K Q 2017 *J. Appl. Phys.* **122** 054302
[185] Zhang Z Q and Lü J T 2017 *Phys. Rev. B* **96** 125432
[186] Wang Z L and Song J H 2006 *Science* **312** 242
[187] Wu W H, Wang L, Li Y L, Zhang F, Lin L, Niu S M, Chenet D, Zhang X, Hao Y F, Heinz T F, Hone J and Wang Z L 2014 *Nature* **514** 470
[188] Wang X D, Song J H, Liu J and Wang Z L 2007 *Science* **316** 102
[189] Wang X F, Dai Y J, Liu R Y, He X, Li S T and Wang Z L 2017 *ACS Nano* **11** 8339
[190] Liu Y Y, Li B L, Zhou W X and Chen K Q 2016 *Appl. Phys. Lett.* **109** 113107